



**HAL**  
open science

## **Utero-placental expression and functional implications of HSD11B1 and HSD11B2 in canine pregnancy**

Miguel Tavares Pereira, Gerhard Schuler, Selim Aslan, Rita Payan-Carreira,  
Iris Reichler, Karine Reynaud, Mariusz Kowalewski

► **To cite this version:**

Miguel Tavares Pereira, Gerhard Schuler, Selim Aslan, Rita Payan-Carreira, Iris Reichler, et al.. Utero-placental expression and functional implications of HSD11B1 and HSD11B2 in canine pregnancy. *Biology of Reproduction*, 2023, 108 (4), pp.645-658. 10.1093/biolre/ioac214 . hal-04235811

**HAL Id: hal-04235811**

**<https://hal.inrae.fr/hal-04235811>**

Submitted on 10 Oct 2023

**HAL** is a multi-disciplinary open access archive for the deposit and dissemination of scientific research documents, whether they are published or not. The documents may come from teaching and research institutions in France or abroad, or from public or private research centers.

L'archive ouverte pluridisciplinaire **HAL**, est destinée au dépôt et à la diffusion de documents scientifiques de niveau recherche, publiés ou non, émanant des établissements d'enseignement et de recherche français ou étrangers, des laboratoires publics ou privés.

1 **Utero-placental expression and functional implications of**  
2 **HSD11B1 and HSD11B2 in canine pregnancy**

3 Miguel Tavares Pereira<sup>1</sup>; Gerhard Schuler<sup>2</sup>; Selim Aslan<sup>3</sup>; Rita Payan-Carreira<sup>4</sup>; Iris M  
4 Reichler<sup>5</sup>; Karine Reynaud<sup>6,7</sup>; Mariusz P Kowalewski<sup>1,8</sup>

5  
6 <sup>1</sup>Institute of Veterinary Anatomy, Vetsuisse Faculty, University of Zurich (UZH), Zurich, Switzerland

7 <sup>2</sup>Clinic for Obstetrics, Gynecology and Andrology of Large and Small Animals, Justus-Liebig-University,  
8 Giessen, Germany

9 <sup>3</sup>Department of Obstetrics and Gynecology, Faculty of Veterinary Medicine, Near East University, Nicosia,  
10 Cyprus

11 <sup>4</sup>School of Science and Technology, Department of Veterinary Medicine, University of Évora, Évora, Portugal

12 <sup>5</sup>Clinic for Reproductive Medicine, Vetsuisse Faculty, University of Zurich (UZH), Zurich, Switzerland

13 <sup>6</sup>École Nationale Vétérinaire d'Alfort, EnvA, 94700 Maisons-Alfort, France

14 <sup>7</sup>Physiologie de la Reproduction et des Comportements, CNRS, IFCE, INRAE, Université de Tours, PRC,  
15 Nouzilly, France

16 <sup>8</sup>Center for Clinical Studies (ZKS), Vetsuisse Faculty, University of Zurich (UZH), Zurich, Switzerland

17

18 **Grant Support**

19 The present work was supported by the Swiss National Science Foundation (SNSF) research  
20 grant number 31003A\_182481.

21

22 **Correspondence:**

23 Prof. Dr. Mariusz P. Kowalewski, PhD

24 Institute of Veterinary Anatomy

25 Vetsuisse Faculty

26 University of Zurich

27 Winterthurerstrasse 260

28 CH-8057 Zurich, Switzerland

29 Tel.: 0041-44-6358784; Fax.: 0041-44-6358943

30 Email: [kowalewski1@yahoo.de](mailto:kowalewski1@yahoo.de) or [kowalewski@vetanat.uzh.ch](mailto:kowalewski@vetanat.uzh.ch)

31

32 **Email addresses:**

33 MTP: [miguel.tavarespereira@uzh.ch](mailto:miguel.tavarespereira@uzh.ch)

34 GS: [Gerhard.Schuler@vetmed.uni-giessen.de](mailto:Gerhard.Schuler@vetmed.uni-giessen.de)

35 RPC: [rtpayan@uevora.pt](mailto:rtpayan@uevora.pt)

36 SA: [selim.aslan@neu.edu.tr](mailto:selim.aslan@neu.edu.tr)

37 IMR: [ireichler@vetclinics.uzh.ch](mailto:ireichler@vetclinics.uzh.ch)

38 KR: [karine.reynaud@inrae.fr](mailto:karine.reynaud@inrae.fr)

39 MPK: [kowalewski@vetanat.uzh.ch](mailto:kowalewski@vetanat.uzh.ch) or [kowalewski1@yahoo.de](mailto:kowalewski1@yahoo.de)

40

41 **Running title**

42 HSD11B1 and -2 expression in the canine placenta

43

44 **Summary Sentence**

45 The canine placenta appears to have increased trophoblast-mediated inactivation of cortisol  
46 during mid-pregnancy, whereas parturition appears to be marked by increased local cortisol  
47 availability.

48

49 **Keywords**

50 dog (*Canis lupus familiaris*), placenta, parturition, cortisol, hydroxysteroid 11-beta  
51 dehydrogenase (HSD11B) 1/2

52

53 **Abstract**

54 Apart from being stress mediators, glucocorticoids modulate the feto-maternal interface during  
55 the induction of parturition. In the dog, the prepartum rise of cortisol in the maternal circulation  
56 appears to be erratic, and information about its contribution to the prepartum luteolytic cascade  
57 is scarce. However, the local placental upregulation of glucocorticoid receptor (GR/NR3C1) at  
58 term led to the hypothesis that species-specific regulatory mechanisms might apply to the  
59 involvement of cortisol in canine parturition. Therefore, here, we assessed the canine  
60 uterine/utero-placental spatio-temporal expression of hydroxysteroid 11-beta dehydrogenase 1  
61 (HSD11B1; reduces cortisone to cortisol), and -2 (HSD11B2; oxidizes cortisol to the inactive  
62 cortisone). Both enzymes were detectable throughout pregnancy, their transcriptional levels  
63 were elevated following implantation, with a strong increase in *HSD11B2* post-implantation  
64 (days 18-25 of pregnancy), and in *HSD11B1* at mid-gestation (days 35-40) ( $P<0.05$ ).”.  
65 Interestingly, when compared pairwise, *HSD11B2* transcripts were higher during post-  
66 implantation, whereas *HSD11B1* dominated during mid-gestation and luteolysis ( $P<0.05$ ). A  
67 custom-made species-specific antibody generated against HSD11B2 confirmed its decreased  
68 expression at prepartum luteolysis. Moreover, in mid-pregnant dogs treated with aglepristone,  
69 *HSD11B1* was significantly higher than -2 ( $P<0.05$ ). HSD11B2 (protein and transcript) was  
70 localized mostly in the syncytiotrophoblast, whereas *HSD11B1* mRNA was mainly localized  
71 in cytotrophoblast cells. Finally, in a functional approach using placental microsomes, a  
72 reduced conversion capacity to deactivate cortisol into cortisone was observed during  
73 prepartum luteolysis, fitting well with the diminished HSD11B2 levels. In particular, the latter  
74 findings support the presence of local increased cortisol availability at term in the dog,  
75 contrasting with an enhanced inactivation of cortisol during early pregnancy.

76

77 **1. Introduction**

78 The adrenal-derived cortisol, besides its association with stress, is involved in biological  
79 processes including reproductive events such as fetal development and the parturition cascade  
80 [1, 2]. Parturition is an orchestrated, mostly species-specific event, involving complex

81 endocrine signaling cascades that are still not fully characterized in several eutherian species.  
82 The sheep is one of the animal species in which the initiation of parturition is well studied and  
83 serves as a translational model for other domestic animal species. Thus, in this animal model,  
84 parturition appears to be triggered by increased amounts of fetal adrenal-derived cortisol [1, 3],  
85 inducing a shift in placental steroidogenic activity towards increased estradiol (E2) production,  
86 replacing the local progesterone (P4) production. This leads to increased secretion of placental  
87 prostaglandin (PG) F<sub>2</sub> $\alpha$ , which stimulates myometrial activity [1, 3]. The luteolytic activity of  
88 cortisol-induced and placenta-derived PGF<sub>2</sub> $\alpha$  plays further important roles in species where the  
89 corpus luteum is, at least in part, the source of P4, e.g., pig, cow, goat, mouse, cat, and rabbit  
90 [4]. Interestingly, in guinea pigs, humans, and other primates, parturition occurs in the presence  
91 of high circulating amounts of P4, accompanied, however, by local, i.e., placental, withdrawal  
92 of P4 signaling [5-8]. Accordingly, several mechanisms, involving local metabolism,  
93 differential expression of P4 receptor (PGR) isoforms, synthesis and availability of lower  
94 activity P4 metabolites, and accessibility of transcription factors, have been implied in the  
95 underlying regulatory mechanisms [s. reviewed in 7, 9]. In addition, the competitive binding  
96 activity observed between the glucocorticoid receptor (GR/NR3C1) and PGR [10, 11] is also  
97 thought to contribute to the functional local withdrawal of P4 in human placenta [12]. In  
98 contrast, cortisol appears to have a low binding capacity to PGR at physiological levels [10,  
99 13].

100 The unique endocrinological features of the dog, when compared with other domestic  
101 mammals, hinder the translation of different parturition-associated biological strategies  
102 observed in other species. The dog is the only domestic mammal in which no steroidogenic  
103 activity is observed in the placenta, with P4 being produced solely by the corpus luteum (CL)  
104 [14, 15]. This further accounts for the absence of a parturition-specific increase of estrogens  
105 [14, 16]. Furthermore, due to the absence of anti-luteolytic mechanisms during early diestrus,  
106 the dog presents an inherently regulated and long lasting activity of the CL [17, 18]. In the  
107 canine endotheliochorial placenta, maternal stroma-derived decidual cells are the only cellular  
108 population expressing the nuclear PGR [19-21]. This distribution of PGR is especially  
109 important when considering the parturition cascade. The prepartum decline of circulating P4  
110 levels, or functional blocking of PGR with antigestagens (e.g., aglepristone), results in  
111 decreased decidual cell-mediated P4/PGR signaling, associated with increased prepartum  
112 production of luteolytic PGF<sub>2</sub> $\alpha$  by the trophoblast, and leading to parturition/abortion [22].

113 Regarding canine cortisol, increased circulating amounts have been reported in dogs at the time  
114 of parturition [14, 23-25]. However, due to wide variation in detected levels, ranging from nadir

115 to clearly measurable values, elevated circulating cortisol levels are not considered a  
116 prerequisite for the induction of parturition in dogs and could be indicative of maternal stress  
117 [14, 23]. Nevertheless, despite its weak clinical applicability (repeated treatments with high  
118 dosages over longer time, associated with strong side effects), the termination of canine  
119 pregnancy can be induced with exogenously-administered glucocorticoids during the last third  
120 of pregnancy [26-28]. Furthermore, GR/NR3C1 was detected in the canine fetal trophoblast,  
121 and was upregulated in the placenta at the time of prepartum luteolysis [29]. Interestingly, in  
122 samples collected after preterm induction of luteolysis with aglepristone, GR/NR3C1  
123 expression remained unaffected, despite the increased PGF $2\alpha$  output observed following  
124 treatment [21]. Jointly, these observations exclude the increased availability of GR/NR3C1 as  
125 a requirement for the prepartum release of PGF $2\alpha$  in the dog [29]. Instead, it was proposed that  
126 GR/NR3C1 could be involved in a P4 withdrawal mechanism [29], similar to its proposed role  
127 in humans [12].

128 Underlying the present project, we hypothesized that glucocorticoids might be involved in the  
129 parturition cascade in the dog, and that their signaling and availability might be regulated  
130 locally in the placenta. Accordingly, recently, changes in the placental transcriptional profile  
131 during parturition were investigated in canine placental samples collected during mid-  
132 pregnancy and at the time of luteolysis, both prepartum and antigestagen-induced (abortion at  
133 mid-term) [30]. Among the differentially expressed genes were factors identified as potentially  
134 modulated by P4, i.a., hydroxysteroid 11-beta dehydrogenase 2 (*HSD11B2*), that, although  
135 being initially abundantly expressed, was downregulated during the termination of pregnancy  
136 [30]. HSD11B2, together with HSD11B1, interconvert the biologically inactive cortisone and  
137 the active cortisol [31]. HSD11B1 is predominantly a reductase, reducing cortisone into  
138 cortisol, and is expressed in several tissues (e.g., liver, adipose tissue and placenta, central  
139 nervous system, cardiovascular system or immune system), where it increases the intracellular  
140 glucocorticoid availability [31, 32]. Moreover, HSD11B1 can act as a dehydrogenase under  
141 specific circumstances, mainly associated with the disruption of cellular activity and/or  
142 metabolic disturbances like diabetes or obesity [31, 32]. In contrast, HSD11B2 acts solely as a  
143 dehydrogenase, decreasing local cortisol availability by converting it into cortisone [31]. The  
144 cortisol-inactivating function of HSD11B2 in the placenta acts as a protective mechanism  
145 against the passage of glucocorticoids into fetal circulation in humans [33]. However, the only  
146 information to date about these factors in the canine placenta is from the transcriptomic study  
147 [30]. To contribute to the knowledge regarding local regulatory mechanisms, and test our  
148 hypothesis regarding the local involvement of cortisol metabolism in the maintenance of canine

149 pregnancy, we investigated the expression and regulation of HSD11B1 and -2 in the canine  
150 uterus and/or placenta throughout pregnancy.

151

## 152 **2. Materials and Methods**

### 153 **2.1 Tissue collection and preservation**

154 Uterine/utero-placental samples from 41 clinically healthy crossbred sexually mature bitches  
155 were collected by routine ovariohysterectomy. Several of these tissue samples originated from  
156 previous studies, where details on animal manipulation and staging of pregnancy are described  
157 [21, 30, 34-37]. Animal experiments were carried out in accordance with animal welfare ethical  
158 principles and legislation, and approved by the responsible ethics committees of the Justus-  
159 Liebig University Giessen, Germany (permits no. II 25.3-19c20- 15c GI 18/14 and VIG3-19c-  
160 20/ 15 GI 18,14); of the University of Ankara, Turkey (permits no. Ankara 2006/06 and 2008-  
161 25- 124); and of the national review board CNREEA #16 (APAFIS #2015042112442132) for  
162 the Alfort Veterinary School (facility 947-046-2), France. Further samples from animals  
163 submitted to routine ovariohysterectomy at the Section of Small Animal Reproduction,  
164 Vetsuisse Faculty, Zurich, were collected after the owners' informed consent.

165 The onset of spontaneous estrus was observed in all animals, with the day of ovulation being  
166 determined when circulating P4 concentration exceeded 5 ng/ml. After the required period for  
167 oocyte maturation in the oviduct, i.e., 2-3 days [17], animals were mated (day 0 of pregnancy).  
168 Uterine or utero-placental samples (depending on the pregnancy stage) were divided in the  
169 following groups: non-pregnant animals (E-, days 8 - 12 after mating, n = 5), pre-implantation  
170 (E+, days 8 - 12 of pregnancy, n = 5), time of implantation (Day 17, n = 4), post-implantation  
171 (Post-Imp, days 18 - 25 of pregnancy, n = 7), mid-gestation (Mid-Gest, days 35 - 40 of  
172 pregnancy, n = 6), prepartum luteolysis (Lut, n = 4), 24h after aglepristone treatment (Agle 24h,  
173 n = 5) and 72h after aglepristone treatment (Agle 72h, n = 5). As implantation takes place at  
174 day 17 [20, 38, 39], confirmation of pregnancy during early pre-implantation period was  
175 performed with embryo flushing (E+). Animals in which no embryos could be retrieved  
176 between days 8 - 12 were allocated to the non-pregnant control group (E-). Samples from the  
177 Lut group were collected during active prepartum P4 decline, determined by hormonal  
178 measurements every 6h until P4 concentrations were below 3 ng/ml in three consecutive  
179 assessments. Aglepristone (Alizine, Virbac, Bad Oldesloe, Germany) was used to induce the  
180 termination of pregnancy in 10 animals at mid-pregnancy (days 40 - 45 after mating), following  
181 the protocol provided by the supplier, i.e., administration of 10 mg/kg body weight twice 24h

182 apart. Samples containing uterine and placental sections were collected 24 or 72h after the  
183 second administration of aglepristone.

184 After surgery, samples were washed with PBS and dissected from connective tissue. Samples  
185 used for RNA and protein analysis were immersed in RNAlater (Ambion Biotechnology  
186 GmbH, Wiesbaden, Germany) at 4°C for 24h and then stored at -80°C until needed. For  
187 histology, samples were fixed in 10% phosphate-buffered formalin for 24h, washed with PBS  
188 for 7 consecutive days, dehydrated in an ethanol series, transferred into xylol and embedded in  
189 paraffin. Whereas all samples were used for TaqMan PCR, 3 samples/group were used for  
190 immunohistochemistry and *in situ* hybridization experiments.

191

## 192 **2.2 RNA isolation, reverse transcription and semi-quantitative real-time TaqMan PCR**

193 The isolation of total RNA was performed with TRIzol reagent (Invitrogen, Varlsbad, CA,  
194 USA), following the supplier's instructions. A NanoDrop 2000 spectrophotometer  
195 (ThermoFisher Scientific AG, Reinach, Switzerland) was used to assess RNA quantity and  
196 purity. For each sample, RNA was cleaned of possible contaminating genomic DNA with the  
197 RQ1 RNA-free DNase kit (Promega, Dübendorf, Switzerland), and reverse transcribed using  
198 the MultiScribe Reverse Transcriptase with random hexamers used as primers (Applied  
199 Biosystems by Thermo Fisher, Foster City, CA, USA); cDNA corresponding to 1.2µg of total  
200 RNA was used per sample and reaction. The relative gene expression was assessed by semi-  
201 quantitative real time TaqMan PCR, following the previously described protocol [40, 41], in  
202 an ABI PRISM 7500 Sequence Detection System fluorometer (Applied Biosystems). All  
203 reactions were run in duplicate with Fast Start Universal Probe Master (Roche Diagnostics AG,  
204 Basel, Switzerland) and gene expression TaqMan assays targeting *HSD11B1*  
205 (Cf02626817\_m1) and *HSD11B2* (Cf02690463\_s1), all obtained from Applied Biosystems.  
206 Autoclaved water and non-reverse transcribed DNase-treated RNA were used as negative  
207 controls. Relative quantification was performed with the comparative Ct method ( $\Delta\Delta Ct$ ),  
208 following logarithmic transformation of values, calibrated to the average expression among all  
209 samples, and normalized to the expression of reference genes. Initially, three reference genes  
210 were evaluated, following our recent description [42]: *PTK2* (Cf02684608\_m1), *EIF4H*  
211 (Cf02713640\_m1) and *KDM4A* (Cf02708629\_m1). The evaluation of the stability of the  
212 reference genes was further assessed with RefFinder [43]. Since *PTK2* and *KDM4A* were more  
213 stable than *EIF4H* in the samples used in this study, these two genes were used for the  $\Delta\Delta Ct$   
214 calculation.

215 For the compartmentalization studies, formalin-fixed and paraffin-embedded (FFPE) utero-  
216 placental samples from 3 animals belonging to Mid-Gest or Lut groups were used, according  
217 to our previously described protocol [29, 44]. A total of 3 tissue sections per animal were cut  
218 with 5 µm thickness and mounted on Arcturus PEN membrane glass slides (LCM0522, Applied  
219 Biosystems). Tissue sections were then deparaffinized, rehydrated, stained with hematoxylin  
220 for histological visualization and dried overnight at 37°C. Using a stereomicroscope, the  
221 different utero-placental compartments (i.e., placental labyrinth, endometrium and  
222 myometrium) were identified and dissected with sterile scalpel blades. Total RNA was isolated  
223 using the RNeasy FFPE Kit (Qiagen GmbH, Hilden, Germany), following the manufacturer's  
224 protocol, and RNA concentration was measured with a NanoDrop 2000. Following the variable,  
225 and sometimes low, yield of RNA obtained from these samples (ranging 43 to 416 ng/µl), 10  
226 ng of RNA were DNase treated and reverse transcribed with the High Capacity cDNA Reverse  
227 Transcription Kit (Applied Biosystems). Afterwards, the obtained cDNA was amplified with  
228 the TaqMan PreAmp Master Mix kit, following the supplier's protocols and as previously  
229 described [40]. For this, TaqMan assays for *HSD11B1*, *HSD11B2* and reference genes were  
230 pooled and mixed with the previously prepared cDNA and TaqMan Preamp Master Mix.  
231 Samples were then amplified using an Eppendorf Mastercycler (Vaudax-Eppendorf AG, Basel,  
232 Switzerland). Following this, the semi-quantitative PCR and relative gene expression  
233 quantification was performed as described above.

234

### 235 **2.3 Immunohistochemistry (IHC)**

236 Since no species-specific or cross-reacting antibodies were commercially available for the  
237 canine species, the development of polyclonal antibodies was attempted, as previously  
238 described [44], and was successful for generating a custom-made anti-HSD11B2 antibody (but  
239 not for HSD11B1) (Eurogentec Seraing, Belgium). Therefore, guinea pigs were immunized  
240 using the peptide sequence C+RALRPGQPGSTPAQ (aa 270-284) and  
241 C+LAAQPRRRYYPGRGL (aa226-240), based on the available sequences (GenBank  
242 accession number XM\_005620822.3). Cysteine (C+) was added to the N-terminal to allow  
243 peptide conjugation to carrier proteins, and the NH<sub>2</sub>-terminus was added to the C-end of the  
244 peptide to mimic the uncharged peptide bond in the protein. After preliminary assessments of  
245 IHC staining, the affinity purified antibody targeting the sequence C+RALRPGQPGSTPAQ  
246 was used in further analyses.

247 The standard indirect immunoperoxidase method was used for IHC to localize the expression  
248 of HSD11B2 protein in the canine placenta during post-implantation, mid-gestation and



249 prepartum luteolysis. Additionally, to allow for better differentiation between cell types,  
250 consecutively cut slides from mid-gestation animals were stained against the endothelin  
251 receptor B (goat polyclonal anti-EDNRB, sc-21196, Santa Cruz Biotechnology), staining for  
252 syncytiotrophoblast [45], and nuclear progesterone receptor (mouse monoclonal anti-PGR,  
253 IM1408, Beckman Coulter Life Sciences, Indianapolis, IN, USA), staining for decidual cells  
254 [21]. IHC was performed as previously described [40, 41]. Sections with 3  $\mu$ m of FFPE tissue  
255 samples were mounted on microscope slides (SuperFrost; Menzel-Glaeser, Braunschweig,  
256 Germany), deparaffinized and rehydrated. Antigen retrieval was performed by heating in a  
257 microwave oven with Tris-EDTA buffer (10mM Tris base + 1mM EDTA solution, pH = 9, for  
258 HSD11B2) or 10mM citrate buffer (pH = 6, for PGR and EDNRB). After quenching  
259 endogenous peroxidase activity with 0.3% hydrogen peroxidase in methanol, slides were  
260 incubated in 10% goat or horse serum (depending on the secondary antibody) to decrease  
261 nonspecific binding, and then incubated overnight at 4°C with primary antibodies at the  
262 following dilutions: anti-HSD11B2 diluted at 1:1000; anti-PGR at 1:100.; EDNRB at 1:200.  
263 Pre-immune serum (in the case of HSD11B2) or non-immune IgG (in the case of PGR and  
264 EDNRB) were used as negative/isotype controls (goat IgG I-5000, and mouse IgG I-2000, both  
265 from Vector Laboratories Inc., Burlingame, CA, USA), at the same protein concentration as the  
266 primary antibodies. Following the incubation with a biotinylated secondary antibody diluted at  
267 1:100 (BA-7000 goat anti-guinea pig for HSD11B2; BA-9500 horse anti-goat IgG for EDNRB;  
268 BA-2000 horse anti-mouse IgG for PGR; all from Vector Laboratories Inc.) and with  
269 streptavidin-peroxidase ABC kit (Vector Laboratories Inc.), positive signals were revealed with  
270 the Liquid DAB+ substrate kit (Dako Schweiz AG, Baar, Switzerland). Slides were then  
271 counterstained with haematoxylin, dehydrated and mounted with Histokit (Assistant, Osterode,  
272 Germany). The localization of positive signals and capture of representative pictures were  
273 performed with a Leica DMRXE light microscope equipped with a Leica Flexacam C1 camera  
274 (Leica Microsystems, Wetzlar, Germany).

275

#### 276 **2.4 *In situ* hybridization (ISH)**

277 As the coding sequence available for canine *HSD11B2* in GenBank was only predicted,  
278 molecular cloning was performed to confirm the sequence and generate templates for cRNA to  
279 be used in ISH. Therefore, the following primers were used: forward: 5'-CCA AGA AGC TAG  
280 ATG CCA TG-3', reverse: 5'-CCT GTG GGC ACT GCT CAT T-3' (ordered from Microsynth  
281 AG, Balgach, Switzerland), generating amplicons of 937 bp. Hot start PCR was applied with  
282 AmpliTaq Gold DNA polymerase (Applied Biosystems) using two uterine cDNA samples;

283 annealing temperature was set at 58°C. PCR products were separated on a 2% agarose gel  
284 stained with ethidium bromide and isolated using the QIAquick Gel Extraction Kit (Qiagen  
285 GmbH). The products were then subcloned into pGEM-T vector (Promega) before  
286 transforming into XL1 Blue competent cells (Stratagene, La Jolla, CA, USA) for multiplication.  
287 Plasmids were isolated with the PureYield Plasmid Miniprep System (Promega), and control  
288 double-digestion was performed with NcoI and NotI restriction enzymes (New England  
289 Biolabs, Frankfurt, Germany). Plasmids were then sent for commercial sequencing (Microsynth  
290 AG). The partial sequence of canine-specific *HSD11B2* was submitted to GenBank with the  
291 accession number.

292 In the next step, the cellular localization of transcripts encoding for both enzymes was assessed  
293 with non-radioactive ISH, following our previously published protocols [21, 46, 47]. Placentae  
294 collected during mid-gestation and parturition luteolysis were used. In addition to the cloned  
295 sequence of *HSD11B2* that was used as a template for generating riboprobes, the canine-  
296 specific *HSD11B1* sequence was available in GenBank: NM\_001005756.1. The following  
297 primers were then used for both targets; *HSD11B1* for: 5'-GCA GAA GCA TGG AAG TCA  
298 AC-3', rev: 5'-TGA GGC CGA GGA TAC AGA G-3', 251 bp; and *HSD11B2* for: 5'- ACC  
299 TCA GCC CAG TCG TAG AT-3', rev: 5'- AGG GCC TTC ATT TGG ATC TGG -3', 248bp  
300 (ordered from Microsynth). The PCR products were then purified and subcloned into pGEM-T  
301 plasmids following the protocol described above. The specificity and identification of sense  
302 and anti-sense direction of products in the plasmid was performed by commercial sequencing  
303 of plasmids single cut with either NcoI or NotI restriction enzymes (Microsynth AG), and  
304 cRNA probes labelled with digoxigenin (DIG) were synthesized using the DIG-RNA Labelling  
305 Kit (Roche Diagnostics AG). The efficiency of riboprobes synthesis was confirmed with a dot-  
306 blot analysis, evaluating signal intensity in serial dilutions of the probes in positively charged  
307 nylon membranes stained against DIG (Roche Diagnostics AG). In the next step, tissue sections  
308 of 2 µm thickness were mounted on microscope slides, deparaffinized in xylene, rehydrated,  
309 digested with 70 µg/ml proteinase K for 19 mins at 37°C (Sigma-Aldrich Chemie GmbH) and  
310 post-fixed with 4% paraformaldehyde. *In situ* hybridization of cRNA probes was performed  
311 overnight at 37°C in the presence of formamide. Sense probes served as negative controls. After  
312 blocking of nonspecific signals with 3% ovine serum, samples were incubated overnight with  
313 alkaline phosphatase-conjugated sheep anti-DIG Fab Fragments diluted 1:5000 (Roche  
314 Diagnostics AG). Endogenous alkaline phosphatase signals were blocked with levamisole.  
315 Detection of positive signals was performed with 5-bromo-4-chloro-3-indolyl phosphate and  
316 nitroblue tetrazolium (BCIP/NBT, Roche Diagnostics AG). Representative pictures were

317 obtained with a Leica DMRXE light microscope equipped with a Leica Flexacam C1 camera  
318 (Leica Microsystems).

319

## 320 **2.5 Protein extraction and western blot**

321 The relative protein expression of HSD11B2 was assessed, following our previously published  
322 protocols [35, 48]. Randomly selected utero-placental samples from post-implantation, mid-  
323 gestation and parturition luteolysis groups (n = 3/group) were homogenized in lysis buffer (Net2  
324 Buffer: 50 mM Tris-HCl, pH = 7.4, 300 mM NaCl, 0.05% NP-40; containing 10µl/ml of  
325 protease inhibitor cocktail) on using an IKA Euro-ST D overhead stirrer (IKA-Werke GmbH,  
326 Staufen, Germany). Samples were then centrifuged (10 min at 10,000 g) and the protein content  
327 of the supernatants was then quantified with the Bradford assay using a SmartSpec Plus  
328 spectrophotometer (Bio-Rad Laboratories, Munich, Germany). Protein samples were  
329 normalized with a sample buffer (25 mM Tris-Cl, pH = 6.8, containing 1% SDS, 5% β-  
330 mercaptoethanol, 10% glycerol and 0.01% bromophenol blue), and 20 µg of protein from each  
331 sample were heated at 95°C for 10 min, followed by electrophoresis separation in a 10%  
332 polyacrylamide gel (AppliChem GmbH, Darmstadt, Germany). Proteins were then transferred  
333 into a methanol-activated polyvinylidene difluoride (PVDF) membrane (Bio-Rad  
334 Laboratories). Non-specific binding sites were blocked with 5% low-fat powdered milk diluted  
335 in PBST (PBS + 0.25% Tween-20), and membranes were incubated overnight at 4°C with anti-  
336 HSD11B2 antibody diluted at 1:250 in 2.5% low-fat powdered milk in PBST solution.  
337 Membranes were then incubated with a rabbit anti-guinea pig horseradish peroxidase (HRP)-  
338 conjugated antibody (1: 15000, A5545, Sigma Aldrich Chemie GmbH, Buchs, Switzerland),  
339 followed by the detection of signals with the SuperSignalWest Chemiluminescent Kit substrate  
340 (Thermo Fisher Scientific AG, Reinach, Switzerland) in a Chemi-Doc XRS+ System and Image  
341 Lab Software (Bio-Rad Laboratories). To ensure specificity, anti-HSD11B2 antibody was  
342 incubated for 1h at ambient temperature with the immunization peptide (blocking peptide) at  
343 the same dilution, before being used to blot the membrane. For loading control and relative  
344 quantification, PVDF membranes were re-blotted with mouse monoclonal antibody against  
345 ACTINB (1:1000, sc-69879, Santa Cruz Biotechnology, Santa Cruz, CA, USA), followed by a  
346 goat anti-mouse HRP-labelled secondary antibody (1: 15000, W402B, Promega). The optical  
347 density of bands was measured with ImageJ software (US National Institutes of Health,  
348 Bethesda, Maryland, USA). Relative protein expression was calculated by normalizing the  
349 optical density of HSD11B2 against ACTINB in the reblotted membranes and is presented as  
350 standardized optical density (SOD).

351

## 352 **2.6 Evaluation of uteroplacental cortisol-cortisone conversion capacity**

353 To evaluate the capacity of placental tissue to interconvert cortisol and cortisone, microsomal  
354 fractions (crude endoplasmic reticulum) were isolated from utero-placental sections collected  
355 during the post-implantation period, as well as from placenta and endometrium, and myometrial  
356 samples (macroscopically dissected) at the time of prepartum luteolysis (n = 4/group). This was  
357 done using the Endoplasmic Reticulum Isolation Kit (Sigma Aldrich Chemie GmbH),  
358 according to the manufacturer's directions and as previously described [49].

359 All conversion capacity assays were performed blinded, using incubation protocols modified  
360 after [49, 50]. Reaction mixtures (100  $\mu$ l volume) were created by combining 50  $\mu$ l of  
361 microsomal fractions with co-factors and substrates. For the cortisol to cortisone conversion  
362 assay, 0.25 mM NAD<sup>+</sup> (Roche Diagnostics, Mannheim, Germany) was used as co-factor, and  
363 substrate was 25 nM of unlabeled cortisol (Merk KGaA, Darmstadt, Germany) and 1.82 nM  
364 (20 000 cpm) of tritium-labeled [1,2,6,7-<sup>3</sup>H(N)]-cortisol (PerkinElmer LAS GmbH, Rodgau,  
365 Germany). For the cortisone to cortisol conversion assay, the co-factor was 0.25 mM NADPH  
366 +H<sup>+</sup> (Roche Diagnostics), while the substrates were 25 nM of unlabeled cortisone (Merk  
367 KGaA) and 7.5 nM (60 000 cpm) of tritium-labeled [1,2-<sup>3</sup>H(N)]-cortisone (PerkinElmer LAS  
368 GmbH). The use of a mixture of unlabeled and <sup>3</sup>H-labeled substrates was performed to  
369 minimize radioactive waste, while still allowing the evaluation of conversion rates. Mixtures  
370 using random samples were initially incubated for 0, 5, 10, 20 and 30 mins at 37°C to determine  
371 the ideal incubation time. An incubation time of 20 mins was considered the most suitable time  
372 by showing the maximal conversion capacity of the mixture, and was then used for all  
373 subsequent experiments. After incubation was complete, samples were extracted with ethyl  
374 acetate, dried in a MicroDancer infrared vortex-evaporator (Hettich AG, Baech, Switzerland)  
375 and redissolved in 100  $\mu$ l of HPLC mobile phase (methanol/acetonitrile/water 43:3:54 v/v/v).  
376 Samples were then separated via HPLC, following the protocol described in [51]. In short, 20  
377  $\mu$ l of dissolved extracts were separated on a 150  $\times$  4 mm Eurospher II 100-5 C18 reversed-phase  
378 column in a Smartline Manager 5050 and Pump 150 HPLC system (all HPLC equipment from  
379 Knauer, Berlin, Germany) at a flow rate of 1 mL/min. Eluted fractions with 0.5 ml were then  
380 collected and evaporated. The <sup>3</sup>H-activity in HPLC fractions was then measure by adding the  
381 scintillation cocktail Rotiszint eco plus (Carl Roth GmbH, Karlsruhe, Germany) in a Tri-Carb  
382 2810 TR  $\beta$ -scintillation counter (PerkinElmer LAS GmbH). Differentiation between substrate  
383 and metabolite was based on a comparison of retention times with authentic tritiated standards.  
384 The percent of substrate conversion was calculated from the distribution of <sup>3</sup>H activity among

385 the peaks after subtracting technical background of  $\beta$ -scintillation counter and baseline  
386 correction.

387

## 388 **2.7 Statistical analysis**

389 Statistical evaluation of changes in relative transcript levels (relative gene expression, RGE)  
390 and protein amounts (standardized optic density, SOD) between different stages of pregnancy  
391 was performed by one-way ANOVA, followed by Tukey-Kramer multiple comparisons post-  
392 test. In addition, two-tailed unpaired Student's t-test was performed to evaluate possible  
393 differences in pairwise comparisons, i.e. between mRNA amounts of *HSD11B1* and -2 in  
394 different groups. The software GraphPad 2.06 (GraphPad Software Inc, San Diego, CA, USA)  
395 was used for this analysis and  $P < 0.05$  was considered as statistically significant.

396

## 397 **3. Results**

### 398 **3.1 Uterine/utero-placental gene expression during pregnancy**

399 The transcriptional availability of *HSD11B1* and -2 was evaluated in all uterine/utero-placental  
400 tissue samples. The mRNA availability of *HSD11B1* was significantly higher at mid-gestation,  
401 when compared with all earlier stages of pregnancy, and non-pregnant (E-) uterine samples ( $P$   
402  $< 0.001$ , Fig. 1A). There was a high variation in *HSD11B1* expression during luteolysis,  
403 yielding no significant difference between mid-gestation and luteolysis ( $P > 0.05$ , Fig. 1A).  
404 Yet, in antigestagen-induced luteolysis/abortion, the expression of *HSD11B1* was significantly  
405 increased 24 h after mid-pregnant animals were treated with aglepristone ( $P < 0.05$ , Fig. 1B).  
406 The availability of *HSD11B2* mRNA was the highest in post-implantation and mid-gestation  
407 samples, when compared with all other evaluated stages ( $P < 0.05$ , Fig. 1C). In contrast with  
408 *HSD11B1*, the expression of *HSD11B2* was downregulated in samples collected 24 and 72 h  
409 after aglepristone treatment ( $P < 0.05$ , Fig. 1D), resembling the pattern observed during normal  
410 luteolysis. In a pairwise comparison of both enzymes in canine uterine and utero-placental  
411 samples, *HSD11B2* expression was significantly higher than -1 during post-implantation ( $P <$   
412  $0.001$ , Fig. 1E). This changed during mid-gestation and prepartum luteolysis, with *HSD11B1*  
413 transcripts being more abundant than *HSD11B2* ( $P < 0.01$  and  $P < 0.05$ , respectively, Fig. 1E).  
414 A higher expression of *HSD11B1* than *HSD11B2* was further observed in animals treated with  
415 aglepristone ( $P < 0.01$ , Fig. 1F).

416

### 417 **3.2 Compartmentalization of *HSD11B1* and -2 mRNA in the canine uterus**

418 The mRNA abundance of all factors in different tissue layers, i.e., placental labyrinth,  
419 endometrium or myometrium, was assessed in utero-placental units collected during mid-  
420 gestation (i.e., in the mature fully developed placenta) and prepartum luteolysis. The  
421 availability of both *HSD11B1* and *HSD11B2* transcripts was frequently below detection limits  
422 in the myometrium of animals at mid-gestation resulting in the exclusion of these samples from  
423 the statistical evaluation. (Fig. 2). Due to high individual variability, no significant differences  
424 were observed for the expression of *HSD11B1* between the tissue compartments at mid-  
425 gestation ( $P > 0.05$ ). This contrasted with its expression during prepartum luteolysis, with the  
426 placenta showing significantly higher levels than endometrium or myometrium ( $P < 0.05$ , Fig.  
427 2A), suggesting the placenta as being the major source. *HSD11B2* transcripts were significantly  
428 more abundant in the mid-gestation placenta compared with mid-gestation endometrium ( $P <$   
429  $0.01$ ), and with the placental labyrinth and myometrium of prepartum luteolysis ( $P < 0.001$  and  
430  $P < 0.01$ , respectively, Fig. 2B). Furthermore, endometrial availability of *HSD11B2* was  
431 significantly higher than in the placenta during prepartum luteolysis ( $P < 0.05$ , Fig. 2B).

432

### 433 **3.3 Protein expression of HSD11B2 in the canine utero-placental unit**

434 The canine-specific anti-HSD11B2 antibody allowed the detection of a band close to the  
435 predicted protein size (44kDa) in western blot analysis (Fig. 3A). The signal was quenched with  
436 antibody pre-incubated with the immunization peptide (Fig. 3A). In utero-placental  
437 homogenates, HSD11B2 protein expression was significantly higher at post-implantation than  
438 mid-gestation and prepartum luteolysis ( $P < 0.01$  and  $P < 0.001$ , respectively, Fig. 3B),  
439 mirroring the time-dependent changes observed at the mRNA level.

440

### 441 **3.4 Localization of HSD11B1 and HSD11B2 in the canine placenta**

442 The availability of custom-made anti-HSD11B2 antibody has made it possible to study its  
443 expression at both the protein and RNA level, whereas the localization of HSD11B1 was  
444 possible only by applying ISH.

445 During post-implantation, HSD11B2 was predominantly localized at the embryo-maternal  
446 interface of the developing placenta, in invading cytotrophoblast cells (Fig. 4A, left panels). In  
447 the mature placenta, during mid-gestation, signals were mostly localized in the  
448 syncytiotrophoblast, with some weaker staining in other cellular components (e.g. decidual  
449 cells or endothelial cells (Fig. 4A, center panels)). At prepartum luteolysis, the signals were  
450 weaker and a more diffuse staining pattern was observed (Fig. 4A, right panels). The

451 localization of HSD11B2-positive signals in the syncytiotrophoblast was then confirmed in the  
452 mature placenta by performing staining of consecutive slides (Fig. 4B) against PGR, as a  
453 marker of decidual cells [19, 20], and EDNRB, expressed by the syncytiotrophoblast [45].  
454 With ISH, positive signals for *HSD11B1* were mostly localized in cytotrophoblast cells, with  
455 some signals also observed in maternal endothelial cells (Fig. 5A), while for *HSD11B2*, the  
456 signals were mainly observed in the syncytiotrophoblast, with a more diffuse pattern observed  
457 during luteolysis than during mid-gestation, as seen with IHC (Fig. 5B).

458

### 459 **3.5 Enzymatic conversion between cortisol and cortisone in canine placental homogenates**

460 The potential of the placenta to interconvert cortisol and cortisone was evaluated in samples  
461 collected during post-implantation, where a significantly higher mRNA availability of  
462 *HSD11B2* than *-1* was observed, and at the time of parturition luteolysis, where an inverted  
463 pattern, associated with decreased protein expression of HSD11B2, was observed. Due to  
464 difficulties in the separation of intact tissue layers containing the invading trophoblast from  
465 remaining tissue layers in the still developing utero-placental interface at post-implantation, full  
466 tissue cross-sections were used for post-implantation specimens. On the other hand, in the fully  
467 developed placenta at parturition luteolysis, the separation between physiological layers of  
468 placenta with adjacent endometrium from myometrium (the latter presenting low mRNA  
469 availability of both factors, being used as a negative control) was performed at the level of  
470 physiologically significantly enlarged endometrial chambers (i.e., deep endometrial glands).  
471 When evaluating conversion rates, values below 5% were considered as unreliable, as the  
472 presence of impurities or decay of the cortisol tracer, in addition to possible technical  
473 background of the beta counter, can mask weak conversion effects.

474 The conversion of cortisol into cortisone (i.e., inactivation of cortisol, indicating HSD11B2  
475 activity), was significantly higher in utero-placental samples collected at post-implantation,  
476 when compared with the conversion rate observed with microsomes isolated from either the  
477 placenta or myometrium obtained during parturition luteolysis ( $P < 0.05$ , Fig. 6). In contrast,  
478 the conversion of cortisone into cortisol (i.e., activation of cortisol) was undetected in post-  
479 implantation samples and myometrium from luteolysis, or remained below 1% in placental +  
480 endometrium samples collected during luteolysis (not shown).

## 481 **4. Discussion**

482 In the attempt to gain new insights into the utero-placental availability of cortisol in the dog,  
483 we evaluated the expression and localization of cortisol-to-cortisone interconverting enzymes

484 HSD11B1 and -2 in the canine uterus and utero-placental compartments throughout pregnancy.  
485 Both cortisol-regulating enzymes were expressed in all samples. Based on their significantly  
486 lower uterine expression at the pre-implantation stage (E+) and in corresponding non-pregnant  
487 controls (E-), as well as on the day of implantation (day 17), than in later gestational stages,  
488 they appeared to be predominantly associated with placental development and functionality.  
489 Therefore, subsequent analyses focused mainly on stages of pregnancy in which a placenta was  
490 present, i.e., post-implantation, mid-gestation and prepartum luteolysis. Indeed, *in situ*  
491 hybridization analysis of both factors, and immunohistochemical detection of HSD11B2,  
492 localized both enzymes predominantly to the fetal-derived trophoblast cells within the canine  
493 placental labyrinth.

494 The transcriptional availability of *HSD11B1* was the highest at mid-gestation, while *HSD11B2*  
495 mRNA levels were already increased during post-implantation. Therefore, there seemed to be  
496 a higher transcriptional availability of *HSD11B2* than *HSD11B1* associated with early  
497 placentation (post-implantation). An excessive exposure to glucocorticoids can cause  
498 detrimental effects in the establishment of pregnancy and in fetal development in different  
499 species [33, 52, 53]. Several of these effects are associated with disrupted expression of  
500 HSD11B2 [54, 55]. Thus, the cortisol-inactivating capacity of HSD11B2 has been  
501 characterized as a protective barrier against the passage of glucocorticoids into fetal circulation  
502 [33, 56-58]. In humans, e.g., fetal glucocorticoids are 5-10 times lower than maternal  
503 circulatory levels [59]. Although several studies have attempted to measure fetal exposition to  
504 cortisol in the dog using, e.g., puppy hair and claws [60, 61], a clear comparison with maternal  
505 levels is still not available. Nevertheless, it appears plausible that such a protective mechanism  
506 might be present in the dog, too. This hypothesis appears to be further supported by the  
507 microsomes activity assay, where an increased conversion of cortisol into cortisone was  
508 observed in post-implantation samples when compared with luteolysis. With regard to the post-  
509 implantation group, the high variability might be due to individual variations or to time-  
510 dependent changes. Nevertheless, there is a clearly higher capacity for cortisol inactivation  
511 (conversion to cortisone) during post-implantation than at the prepartum luteolysis. Within the  
512 fully developed fetal placental compartment, the strongest HSD11B2-positive signals were  
513 mainly localized in the syncytiotrophoblast. A similar localization pattern was previously  
514 described in mice, with placental HSD11B2 being mainly associated with the trophoblast [62],  
515 as well as in humans, where it was exclusively detected in the syncytiotrophoblast [58, 63].  
516 Interestingly, in sheep, representing a non-invasive type of placentation, *HSD11B2* could be  
517 detected reliably in the trophoblast and endoderm of the conceptus, but not in the uterus,



518 during early pregnancy [64]. Thus, despite the weak signals observed in endothelial and  
519 decidual cells in the present study, the increased cortisol-deactivation, possibly associated with  
520 a protective embryonal mechanism against maternal cortisol, appears to be mainly mediated by  
521 the trophoblast during early fetal development.

522 The progression of pregnancy towards parturition was associated with a decreased utero-  
523 placental expression of HSD11B2, which was confirmed at both the mRNA and protein levels.  
524 This was also reflected in its low activity at prepartum luteolysis based on the microsomal  
525 cortisol conversion rates. In fact, with average conversions of 2% in the placenta and  
526 endometrium, and 1.9% in myometrium (both below the defined 5% threshold), luteolysis  
527 appears to be virtually devoid of cortisol into cortisone conversion activity. The decreased  
528 placental availability of HSD11B2 at term was also highlighted by the assessment of mRNA in  
529 different utero-placental compartments, showing its significantly lowered levels between fully  
530 developed mid-term placenta and prepartum luteolysis. Fitting with these observations was the  
531 lowered *HSD11B2* transcription in antigestagen-treated dogs, emphasizing the P4-dependent  
532 expression of HSD11B2. This supports our previous report using the transcriptomic approach  
533 [30], where *HSD11B2* was described as a downstream factor from P4 signaling. As several  
534 samples used in the present work derived from previous projects, serum samples that could  
535 allow a correlation between placental expression of HSD11B1/2 and circulating cortisol or P4  
536 were not available. Nevertheless, circulating P4 levels are described to a greater extent in the  
537 dog [s. reviewed in 65]. Thus, the time-dependent decrease of HSD11B2 expression appears to  
538 accompany, at least in part, the decreasing P4 circulating levels observed in this species,  
539 including the steep prepartum decline. In ovariectomized mouse, the uterine expression of  
540 *HSD11B2* could be upregulated by P4 administration, and later ablated by the PGR blocker  
541 mifepristone (RU486) [57]. Aglepristone used in our studies is a derivate of mifepristone, both  
542 type II antigestagens, with similarities in its chemical structure and activities related to the PGR  
543 [66]. Cumulatively, the recently postulated association between P4/PGR signaling and  
544 placental *HSD11B2* expression in the dog [30], is substantiated by the present findings, clearly  
545 indicating its importance in the luteolytic cascade.

546 The diffuse staining of HSD11B2 in the prepartum labyrinth could possibly be associated with  
547 its significantly lowered abundance and/or degradation. Conversely, the utero-placental  
548 availability of *HSD11B1* increased from post-implantation to mid-gestation, and remained  
549 unaffected at prepartum luteolysis. This was associated with an apparent shift in the  
550 transcriptional availability of both isoforms, with *HSD11B1* being significantly higher than -2  
551 at term. The ISH allowed the detection of mRNA encoding for *HSD11B1* mainly in the

552 cytotrophoblast, with some signals also identified in maternal endothelial cells during  
553 prepartum luteolysis. These observations suggest that a possible interplay between the cortisol-  
554 deactivating syncytiotrophoblast and cortisol-activating cytotrophoblast could be present in the  
555 canine placenta. For instance, in mice, increased expression of *HSD11B1* can be observed in  
556 late pregnancy in fetal tissue [62], and in humans it is localized in endothelial cells and different  
557 trophoblast populations, but not in the syncytiotrophoblast [67]. As part of the approach  
558 involving microsomal activities, we investigated the potential of the placenta to activate  
559 cortisol, thereby addressing the activity of HSD11B1, which was below reliable detection limits  
560 in the placenta from prepartum luteolysis, and was undetectable in myometrium and in post-  
561 implantation samples. The inclusion of a positive control tissue, which was not possible in this  
562 study, could provide a more definitive answer regarding the lack of cortisol activation. While  
563 the low detection of HSD11B1 activity, and the limitations in protein detection, could be  
564 explained by a low availability of this enzyme in the canine placenta, this remains to be  
565 confirmed. The higher utero-placental transcriptional availability of *HSD11B1* in the  
566 antigestagen treated dogs differed from that observed during normal parturition. A possible  
567 explanation could be in the local stress-related response to acute PGR withdrawal [s. reviewed  
568 in 66]. Despite the still veiled importance of the parturition-associated increase of cortisol  
569 activity in the dog, as mentioned elsewhere, the cortisol-stimulated shift in placental  
570 steroidogenesis described for other species [1, 3], does not apply to the dog [14, 15].  
571 Furthermore, only term, and not aglepristone-induced termination of pregnancy, was associated  
572 with the upregulation of GR/NR3C1 [29]. Nevertheless, the lower HSD11B2 activity appears  
573 to be associated with a locally increased availability of cortisol, possibly embryo-derived. This  
574 local cortisol increase could be an important event in the final maturation of the fetus,  
575 associated, e.g., with the final maturation of fetal organs, like the lung [68]. Still, the  
576 confirmation of such local events is still required, as previous cortisol measurements in the dog  
577 were performed at the circulating level [14, 23-25]. Furthermore, as already stated, termination  
578 of pregnancy in the dog is associated with increased circulating PGF $2\alpha$  levels, deriving from  
579 the trophoblast and involving the 9-keto PGE $2$  reductase (9KPGR)-mediated synthesis from  
580 PGE $2$  [49]. An interplay between PGF $2\alpha$  and cortisol has been described in several instances  
581 [1, 4]. However, the extent to which cortisol directly contributes to the placental PGF $2\alpha$  output  
582 affecting the synthetic cascade of prostaglandins in the dog, including the rising COX2/PTGS2  
583 activity [21], remains to be investigated.

## 584 **5. Conclusions**

585 The results from the present work describe, for the first time, the presence of stage-dependent  
586 cortisol-modulating mechanisms in the canine placenta, mainly associated with the trophoblast.  
587 The higher expression of HSD11B2 in early placentation, associated with the local tissue  
588 potential to inactivate cortisol, might be involved in protective mechanisms of the embryo  
589 against maternal-derived glucocorticoids. The P4-dependent regulation of HSD11B2 is further  
590 substantiated by observation both during normal and induced parturition/abortion. A clear shift  
591 in placental regulation of cortisol activity is apparent at term, with parturition being associated  
592 with an increased *HSD11B1* mRNA availability, and decreased HSD11B2 expression and  
593 cortisol-inactivating activity. An interplay between different trophoblast populations is also  
594 apparent, with HSD11B1 being mainly localized in the cytotrophoblast, where GR/NR3C1 is  
595 also expressed [29], while HSD11B2-positive signals were mainly observed in the  
596 syncytiotrophoblast. Although its definitive role remains still to be defined for the dog, in  
597 accordance with our hypothesis, local cortisol appears to be involved in the termination of  
598 canine pregnancy and deserves more attention in the future.

## 599 **Conflict of interests**

600 The authors declare that they have no conflicts of interest.

601

## 602 **Author's contributions**

603 MTP was involved in developing the concept of the present study, experimental design,  
604 generating data, analysis and interpretation of data and drafting of the manuscript. GS was  
605 involved in the generation, analysis and interpretation of data, and revision of the manuscript.  
606 SA, RPC, IMR and KR were involved in the collection of tissue material, knowledge transfer,  
607 critical discussion and interpretation of data, and revision of the manuscript. MPK designed and  
608 supervised the project, was involved in interpretation of the data, and drafting and revision of  
609 the manuscript. All authors read and approved the final manuscript.

## 610 **Acknowledgements**

611 Authors are thankful to Dr. Sharon Mortimer for the careful editing of the manuscript. The  
612 technical expertise and contributions of Ricardo Fernandez Rubia and Kirstin Skaar are greatly  
613 appreciated. Part of the laboratory work was performed using the logistics at the Center for  
614 Clinical Studies, Vetsuisse Faculty, University of Zurich.

615

616 **Figure legends**

617 **Figure 1. Relative gene expression of HSD11B1 and HSD11B2 in the canine uterus/utero-**  
618 **placental compartment during pregnancy and in response to antigestagens.**

619 Relative gene expression is presented as determined by semi-quantitative real time (TaqMan)  
620 PCR ( $\bar{X}$  +/- SD). (A-D) To evaluate the effects of pregnancy progression, or of preterm  
621 termination of pregnancy with aglepristone, one-way non-parametric ANOVA was applied,  
622 revealing: (A)  $P < 0.0001$ , (B)  $P = 0.0197$ , (C)  $P < 0.0001$  and (D)  $P = 0.0009$ . When  $P < 0.05$ ,  
623 analysis was followed by a Tukey-Kramer multiple comparison post-test. (E, F) Comparison  
624 of relative gene expression between *HSD11B1* and *HSD11B2* at each stage was evaluated by  
625 applying Student's unpaired two-tailed t- test. Bars with asterisks differ at: \*  $P < 0.05$ , \*\*  $P <$   
626  $0.01$ , \*\*\*  $P < 0.001$ . E- = embryo-negative/non-pregnant animals, E+ = embryo-positive/pre-  
627 implantation, day 17 = time of implantation, Post-Imp = post-implantation, Mid-Gest = mid-  
628 gestation.

629

630 **Figure 2. Compartmentalization of HSD11B1 and HSD11B2 relative mRNA levels in the**  
631 **utero-placental tissue during mid-gestation and prepartum luteolysis.** Relative gene

632 expression, presented as  $\bar{X}$  +/- SD, was determined by semi-quantitative real time (TaqMan)  
633 PCR. Samples from 3 animals for each pregnancy stage were used. Differences between all  
634 groups was assessed with one-way non-parametric ANOVA, with  $P = 0.0079$  for HSD11B1  
635 and  $P < 0.0001$  for HSD11B2, followed by a Tukey-Kramer multiple comparison post-test. As  
636 the expression of both factors was frequently below detection limits in myometrium during  
637 mid-gestation, these samples were removed from statistical analysis. Bars with asterisks differ  
638 at: \*  $P < 0.05$ , \*\*  $P < 0.01$ , \*\*\*  $P < 0.001$ .

639

640 **Figure 3. Protein expression of HSD11B2 in utero-placental homogenates. (A)** Epitope-

641 blocking peptide was used to block HSD11B2-specific signal (~44kDa) in protein extract of  
642 utero-placental homogenates. (B) Representative immunoblots for HSD11B2 and ACTINB are  
643 shown. Standardized optical density (SOD) of HSD11B2 signals was measured in proteins  
644 extracted from utero-placental samples collected during post-implantation (Post-Imp), mid-  
645 gestation (Mid-Gest) and prepartum luteolysis. After quantifying HSD11B2 signals,  
646 membranes were re-blotted targeting ACTINB for normalization of signals intensity. SOD are  
647 presented as  $\bar{X}$  +/- SD. One-way non-parametric ANOVA revealed  $p = 0.0005$ , followed by a  
648 Tukey-Kramer multiple comparison post-test.

649

650 **Figure 4. Immunohistochemical localization of HSD11B2 in the canine placental labyrinth**  
651 **at selected stages of pregnancy. (A)** During post-implantation, signals were observed in the  
652 invading trophoblast. In the mature mid-gestation placenta, strong positive signals were  
653 localized in syncytiotrophoblast cells, with weak signals also being observed in other placental  
654 cell populations (e.g. endothelial and decidual cells). Samples collected at the time of parturition  
655 luteolysis appear to present a weaker and more diffuse pattern of staining. **(B)** The localization  
656 of HSD11B2-positive signals in the syncytiotrophoblast of the matured placenta was confirmed  
657 by performing consecutive staining of mid-gestation samples targeting PGR (expressed by  
658 decidual cells) and ETB (expressed by syncytiotrophoblast cells). No staining was observed in  
659 the isotype controls (insets in pictures, at the same magnification). Solid arrow = decidual cell;  
660 open arrow = endothelial cell; closed arrowhead = cytotrophoblast; open arrowhead =  
661 syncytiotrophoblast; asterisk = fetal stroma.

662  
663 **Figure 5. Localization of *HSD11B1* and *HSD11B2* mRNA in the canine placental**  
664 **labyrinth at mid-gestation and parturition luteolysis. (A)** *HSD11B1*-positive signals were  
665 mainly localized in cytotrophoblast and endothelial cells. Signal intensity in endothelial cells  
666 appeared to be stronger at parturition luteolysis than at mid-gestation. **(B)** *HSD11B2* was mainly  
667 expressed in the syncytiotrophoblast during mid-gestation, with a more diffuse pattern being  
668 observed at the time of parturition luteolysis. No staining was observed in the negative controls  
669 (sense probe; insets in pictures, at the same magnification). Open arrow = endothelial cell;  
670 closed arrowhead = cytotrophoblast; open arrowhead = syncytiotrophoblast.

671  
672 **Figure 6. Interconversion rate between cortisol and cortisone performed by canine utero-**  
673 **placental microsomes isolated from different stages of pregnancy.** Microsome conversion  
674 rates of cortisol into cortisone are presented as a percentage. Differences between groups was  
675 assessed with one-way non-parametric ANOVA ( $P = 0.0186$ ), followed by a Tukey-Kramer  
676 multiple comparison post-test. Bars with asterisks differ at: \*  $P < 0.05$ .

677  
678 **5. References**

- 679 1. Whittle, W.L., et al., *Glucocorticoid regulation of human and ovine parturition: the relationship between fetal*  
680 *hypothalamic-pituitary-adrenal axis activation and intrauterine prostaglandin production.* Biol Reprod, 2001. **64**(4):  
681 p. 1019-32.
- 682 2. Cottrell, E.C. and J.R. Seckl, *Prenatal stress, glucocorticoids and the programming of adult disease.* Front Behav  
683 Neurosci, 2009. **3**: p. 19.
- 684 3. Liggins, G.C., et al., *The mechanism of initiation of parturition in the ewe.* Recent Prog Horm Res, 1973. **29**: p. 111-  
685 59.
- 686 4. Schuler, G., R. Fürbass, and K. Klisch, *Placental contribution to the endocrinology of gestation and parturition.*  
687 *Animal Reproduction*, 2018. **15**(Suppl. 1): p. 822-842.

- 688 5. Tulchinsky, D., et al., *Plasma estrone, estradiol, estriol, progesterone, and 17-hydroxyprogesterone in human*  
689 *pregnancy. I. Normal pregnancy.* Am J Obstet Gynecol, 1972. **112**(8): p. 1095-100.
- 690 6. Heap, R.B. and R. Deanesly, *Progesterone in systemic blood and placenta of intact and ovariectomized pregnant*  
691 *guinea-pigs.* J Endocrinol, 1966. **34**(4): p. 417-23.
- 692 7. Mitchell, B.F. and M.J. Taggart, *Are animal models relevant to key aspects of human parturition?* Am J Physiol Regul  
693 Integr Comp Physiol, 2009. **297**(3): p. R525-45.
- 694 8. Nnamani, M.C., et al., *Evidence for independent evolution of functional progesterone withdrawal in primates and*  
695 *guinea pigs.* Evol Med Public Health, 2013. **2013**(1): p. 273-88.
- 696 9. Zakar, T. and F. Hertelendy, *Progesterone withdrawal: key to parturition.* Am J Obstet Gynecol, 2007. **196**(4): p. 289-  
697 96.
- 698 10. Ojasoo, T., et al., *Binding of steroids to the progesterin and glucocorticoid receptors analyzed by correspondence*  
699 *analysis.* J Med Chem, 1988. **31**(6): p. 1160-9.
- 700 11. Philibert, D., et al., *From RU 38486 towards Dissociated Antiglucocorticoid and Antiprogestone.* Frontiers of  
701 Hormone Research, 1991. **19**: p. 1-17.
- 702 12. Karalis, K., G. Goodwin, and J.A. Majzoub, *Cortisol blockade of progesterone: a possible molecular mechanism*  
703 *involved in the initiation of human labor.* Nat Med, 1996. **2**(5): p. 556-60.
- 704 13. Ogle, T.F. and B.K. Beyer, *Steroid-binding specificity of the progesterone receptor from rat placenta.* J Steroid  
705 Biochem, 1982. **16**(2): p. 147-50.
- 706 14. Hoffmann, B., et al., *Investigations on hormonal changes around parturition in the dog and the occurrence of*  
707 *pregnancy-specific non conjugated oestrogens.* Exp Clin Endocrinol, 1994. **102**(3): p. 185-189.
- 708 15. Nishiyama, T., et al., *Immunohistochemical study of steroidogenic enzymes in the ovary and placenta during*  
709 *pregnancy in the dog.* Anat Hist Embryol, 1999. **28**(2): p. 125-129.
- 710 16. Onclin, K., B. Murphy, and J.P. Verstegen, *Comparisons of estradiol, LH and FSH patterns in pregnant and*  
711 *nonpregnant beagle bitches.* Theriogenology, 2002. **57**(8): p. 1957-1972.
- 712 17. Kowalewski, M.P., et al., *The Dog: Nonconformist, Not Only in Maternal Recognition Signaling.* Adv Anat Embryol  
713 Cell Biol, 2015. **216**: p. 215-37.
- 714 18. Kowalewski, M.P., *Selected comparative aspects of canine female reproductive physiology,* in *Encyclopedia of*  
715 *Reproduction,* M.K. Skinner, Editor. 2018, Academic Press. p. 682-691.
- 716 19. Vermeirsch, H., P. Simoens, and H. Lauwers, *Immunohistochemical detection of the estrogen receptor- $\alpha$  and*  
717 *progesterone receptor in the canine pregnant uterus and placental labyrinth.* The Anatomical Record, 2000. **26**.
- 718 20. Kowalewski, M.P., et al., *Canine Endotheliochorial Placenta: Morpho-Functional Aspects.* Adv Anat Embryol Cell Biol,  
719 2021. **234**: p. 155-179.
- 720 21. Kowalewski, M.P., et al., *Canine placenta: a source of prepartal prostaglandins during normal and antiprogestin-*  
721 *induced parturition.* Reproduction, 2010. **139**(3): p. 655-64.
- 722 22. Kowalewski, M.P., M. Tavares Pereira, and A. Kazemian, *Canine conceptus-maternal communication during*  
723 *maintenance and termination of pregnancy, including the role of species-specific decidualization.* Theriogenology,  
724 2020. **150**: p. 329-338.
- 725 23. Concannon, P.W., et al., *Parturition and Lactation in the Bitch: Serum Progesterone, Cortisol and Prolactin.* Biology  
726 of Reproduction, 1978. **19**(5).
- 727 24. Veronesi, M.C., et al., *Correlations among body temperature, plasma progesterone, cortisol and prostaglandin*  
728 *F2alpha of the periparturient bitch.* J Vet Med A Physiol Pathol Clin Med, 2002. **49**(5): p. 264-8.
- 729 25. Olsson, K., et al., *Increased plasma concentrations of vasopressin, oxytocin, cortisol and the prostaglandin F2alpha*  
730 *metabolite during labour in the dog.* Acta Physiol Scand, 2003. **179**(3): p. 281-7.
- 731 26. Zone, M., et al., *Termination of pregnancy in dogs by oral administration of dexamethasone.* Theriogenology, 1995.  
732 **43**(2): p. 487-494.
- 733 27. Wanke, M., et al., *Clinical use of dexamethasone for termination of unwanted pregnancy in dogs.* J Reprod Fertil  
734 Suppl, 1997. **51**: p. 233-8.
- 735 28. Austad, R., A. Lunde, and O.V. Sjaastad, *Peripheral plasma levels of oestradiol-17 beta and progesterone in the bitch*  
736 *during the oestrous cycle, in normal pregnancy and after dexamethasone treatment.* J Reprod Fertil, 1976. **46**(1): p.  
737 129-36.
- 738 29. Gram, A., et al., *Elevated utero/placental GR/NR3C1 is not required for the induction of parturition in the dog.*  
739 Reproduction, 2016. **152**(4): p. 303-11.
- 740 30. Nowak, M., et al., *Gene expression profiling of the canine placenta during normal and antigestagen-induced*  
741 *luteolysis.* Gen Comp Endocrinol, 2019. **282**: p. 113194.
- 742 31. Chapman, K., M. Holmes, and J. Seckl, *11beta-hydroxysteroid dehydrogenases: intracellular gate-keepers of tissue*  
743 *glucocorticoid action.* Physiol Rev, 2013. **93**(3): p. 1139-206.
- 744 32. Seckl, J.R. and B.R. Walker, *Minireview: 11beta-hydroxysteroid dehydrogenase type 1- a tissue-specific amplifier of*  
745 *glucocorticoid action.* Endocrinology, 2001. **142**(4): p. 1371-6.
- 746 33. Seckl, J.R. and M.J. Meaney, *Glucocorticoid programming.* Ann N Y Acad Sci, 2004. **1032**: p. 63-84.
- 747 34. Kowalewski, M.P., et al., *Luteal and placental function in the bitch: spatio-temporal changes in prolactin receptor*  
748 *(PRLr) expression at dioestrus, pregnancy and normal and induced parturition.* Reproductive Biology and  
749 Endocrinology, 2011. **9**(109).
- 750 35. Gram, A., A. Boos, and M.P. Kowalewski, *Uterine and placental expression of canine oxytocin receptor during*  
751 *pregnancy and normal and induced parturition.* Reprod Domest Anim, 2014. **49 Suppl 2**: p. 41-9.

- 752 36. Kowalewski, M.P., et al., *Time related changes in luteal prostaglandin synthesis and steroidogenic capacity during pregnancy, normal and antiprogesterin induced luteolysis in the bitch*. Anim Reprod Sci, 2009. **116**(1-2): p. 129-38.
- 753 37. Graubner, F.R., et al., *Decidualization of the canine uterus: From early until late gestational in vivo morphological observations, and functional characterization of immortalized canine uterine stromal cell lines*. Reprod Domest Anim, 2017. **52 Suppl 2**: p. 137-147.
- 754 38. Concannon, P.W., J.P. McCann, and M. Temple, *Biology and endocrinology of ovulation, pregnancy and parturition in the dog*. J Reprod Fertil Suppl, 1989. **39**(0449-3087 ): p. 3-25.
- 755 39. Amoroso, E.C., *Placentation*, in *Marshall's Physiology of Reproduction*, A.S. Parkes, Editor. 1952, Longmans, Greens and Co: London, UK.
- 756 40. Tavares Pereira, M., et al., *Prostaglandin-mediated effects in early canine corpus luteum: in vivo effects on vascular and immune factors*. Reprod Biol, 2019. **19**(1): p. 100-111.
- 757 41. Kowalewski, M.P., et al., *Expression of cyclooxygenase 1 and 2 in the canine corpus luteum during diestrus*. Theriogenology, 2006. **66**(6-7): p. 1423-30.
- 758 42. Nowak, M., S. Aslan, and M.P. Kowalewski, *Determination of novel reference genes for improving gene expression data normalization in selected canine reproductive tissues - a multistudy analysis*. BMC Vet Res, 2020. **16**(1): p. 440.
- 759 43. Xie, F., et al., *miRDeepFinder: a miRNA analysis tool for deep sequencing of plant small RNAs*. Plant Molecular Biology, 2012. **80**(1): p. 75-84.
- 760 44. Nowak, M., et al., *Functional implications of the utero-placental relaxin (RLN) system in the dog throughout pregnancy and at term*. Reproduction, 2017. **154**(4): p. 415-431.
- 761 45. Gram, A., A. Boos, and M.P. Kowalewski, *Cellular localization, expression and functional implications of the utero-placental endothelin system during maintenance and termination of canine gestation*. 2017.
- 762 46. Kowalewski, M.P., et al., *Characterization of the canine 3beta-hydroxysteroid dehydrogenase and its expression in the corpus luteum during diestrus*. J Steroid Biochem Mol Biol, 2006. **101**(4-5): p. 254-62.
- 763 47. Tavares Pereira, M., et al., *Luteal expression of factors involved in the metabolism and sensitivity to oestrogens in the dog during pregnancy and in non-pregnant cycle*. Reprod Domest Anim, 2021.
- 764 48. Gram, A., et al., *Biosynthesis and degradation of canine placental prostaglandins: prepartum changes in expression and function of prostaglandin F2alpha-synthase (PGFS, AKR1C3) and 15-hydroxyprostaglandin dehydrogenase (HPGD)*. Biol Reprod, 2013. **89**(1): p. 2.
- 765 49. Gram, A., et al., *Canine placental prostaglandin E2 synthase: expression, localization, and biological functions in providing substrates for prepartum PGF2alpha synthesis*. Biol Reprod, 2014. **91**(6): p. 154.
- 766 50. Li, X., et al., *Effects of Ziram on Rat and Human 11beta-Hydroxysteroid Dehydrogenase Isoforms*. Chem Res Toxicol, 2016. **29**(3): p. 398-405.
- 767 51. Turpeinen, U., et al., *Determination of urinary free cortisol by HPLC*. Clin Chem, 1997. **43**(8 Pt 1): p. 1386-91.
- 768 52. Jafari, Z., et al., *The Adverse Effects of Auditory Stress on Mouse Uterus Receptivity and Behaviour*. Sci Rep, 2017. **7**(1): p. 4720.
- 769 53. Li, Q.N., et al., *Glucocorticoid exposure affects female fertility by exerting its effect on the uterus but not on the oocyte: lessons from a hypercortisolism mouse model*. Hum Reprod, 2018. **33**(12): p. 2285-2294.
- 770 54. Rogers, S.L., et al., *Diminished 11beta-hydroxysteroid dehydrogenase type 2 activity is associated with decreased weight and weight gain across the first year of life*. J Clin Endocrinol Metab, 2014. **99**(5): p. E821-31.
- 771 55. Belkacemi, L., et al., *Altered placental development in undernourished rats: role of maternal glucocorticoids*. Reprod Biol Endocrinol, 2011. **9**: p. 105.
- 772 56. Togher, K.L., et al., *Epigenetic regulation of the placental HSD11B2 barrier and its role as a critical regulator of fetal development*. Epigenetics, 2014. **9**(6): p. 816-22.
- 773 57. Zheng, H.T., et al., *Progesterone-regulated Hsd11b2 as a barrier to balance mouse uterine corticosterone*. J Endocrinol, 2020. **244**(1): p. 177-187.
- 774 58. Zhu, P., et al., *Mechanisms for establishment of the placental glucocorticoid barrier, a guard for life*. Cell Mol Life Sci, 2019. **76**(1): p. 13-26.
- 775 59. Beitins, I.Z., et al., *The Metabolic Clearance Rate, Blood Production, Interconversion and Transplacental Passage of Cortisol and Cortisone in Pregnancy Near Term*. Pediatric Research, 1973. **7**(5): p. 509-519.
- 776 60. Fusi, J., et al., *The usefulness of claws collected without invasiveness for cortisol and dehydroepiandrosterone (sulfate) monitoring in healthy newborn puppies after birth*. Theriogenology, 2018. **122**: p. 137-143.
- 777 61. Groppetti, D., et al., *Maternal and neonatal canine cortisol measurement in multiple matrices during the perinatal period: A pilot study*. PLoS One, 2021. **16**(7): p. e0254842.
- 778 62. Thompson, A., V.K. Han, and K. Yang, *Spatial and temporal patterns of expression of 11beta-hydroxysteroid dehydrogenase types 1 and 2 messenger RNA and glucocorticoid receptor protein in the murine placenta and uterus during late pregnancy*. Biol Reprod, 2002. **67**(6): p. 1708-18.
- 779 63. Krozowski, Z., et al., *Immunohistochemical localization of the 11 beta-hydroxysteroid dehydrogenase type II enzyme in human kidney and placenta*. J Clin Endocrinol Metab, 1995. **80**(7): p. 2203-9.
- 780 64. Simmons, R.M., et al., *HSD11B1, HSD11B2, PTGS2, and NR3C1 expression in the peri-implantation ovine uterus: effects of pregnancy, progesterone, and interferon tau*. Biol Reprod, 2010. **82**(1): p. 35-43.
- 781 65. Kowalewski, M.P., *Luteal regression vs. prepartum luteolysis: regulatory mechanisms governing canine corpus luteum function*. Reprod Biol, 2014. **14**(2): p. 89-102.
- 782 66. Kowalewski, M.P., et al., *Progesterone receptor blockers: historical perspective, mode of function and insights into clinical and scientific applications*. Tierarztl Prax Ausg K Kleintiere Heimtiere, 2020. **48**(6): p. 433-440.
- 783
- 784
- 785
- 786
- 787
- 788
- 789
- 790
- 791
- 792
- 793
- 794
- 795
- 796
- 797
- 798
- 799
- 800
- 801
- 802
- 803
- 804
- 805
- 806
- 807
- 808
- 809
- 810
- 811
- 812
- 813
- 814
- 815

- 816 67. Sun, K., K. Yang, and J.R. Challis, *Differential expression of 11 beta-hydroxysteroid dehydrogenase types 1 and 2 in*  
817 *human placenta and fetal membranes.* J Clin Endocrinol Metab, 1997. **82**(1): p. 300-5.  
818 68. Bolt, R.J., et al., *Glucocorticoids and lung development in the fetus and preterm infant.* Pediatr Pulmonol, 2001.  
819 **32**(1): p. 76-91.  
820



1 **Utero-placental expression and functional implications of**  
2 **HSD11B1 and HSD11B2 in canine pregnancy**

3 Miguel Tavares Pereira<sup>1</sup>; Gerhard Schuler<sup>2</sup>; Selim Aslan<sup>3</sup>; Rita Payan-Carreira<sup>4</sup>; Iris M  
4 Reichler<sup>5</sup>; Karine Reynaud<sup>6,7</sup>; Mariusz P Kowalewski<sup>1,8</sup>

5  
6 <sup>1</sup>Institute of Veterinary Anatomy, Vetsuisse Faculty, University of Zurich (UZH), Zurich, Switzerland  
7 <sup>2</sup>Clinic for Obstetrics, Gynecology and Andrology of Large and Small Animals, Justus-Liebig-University,  
8 Giessen, Germany  
9 <sup>3</sup>Department of Obstetrics and Gynecology, Faculty of Veterinary Medicine, Near East University, Nicosia,  
10 Cyprus  
11 <sup>4</sup>School of Science and Technology, Department of Veterinary Medicine, University of Évora, Évora, Portugal  
12 <sup>5</sup>Clinic for Reproductive Medicine, Vetsuisse Faculty, University of Zurich (UZH), Zurich, Switzerland  
13 <sup>6</sup>École Nationale Vétérinaire d'Alfort, EnvA, 94700 Maisons-Alfort, France  
14 <sup>7</sup>Physiologie de la Reproduction et des Comportements, CNRS, IFCE, INRAE, Université de Tours, PRC,  
15 Nouzilly, France  
16 <sup>8</sup>Center for Clinical Studies (ZKS), Vetsuisse Faculty, University of Zurich (UZH), Zurich, Switzerland  
17

18 **Grant Support**

19 The present work was supported by the Swiss National Science Foundation (SNSF) research  
20 grant number 31003A\_182481.

21  
22 **Correspondence:**

23 Prof. Dr. Mariusz P. Kowalewski, PhD  
24 Institute of Veterinary Anatomy  
25 Vetsuisse Faculty  
26 University of Zurich  
27 Winterthurerstrasse 260  
28 CH-8057 Zurich, Switzerland  
29 Tel.: 0041-44-6358784; Fax.: 0041-44-6358943  
30 Email: [kowalewski@vetanat.uzh.ch](mailto:kowalewski@vetanat.uzh.ch) or [kowalewski@yahoo.de](mailto:kowalewski@yahoo.de)

31  
32 **Email addresses:**

33 MTP: [miguel.tavarespereira@uzh.ch](mailto:miguel.tavarespereira@uzh.ch)  
34 GS: [Gerhard.Schuler@vetmed.uni-giessen.de](mailto:Gerhard.Schuler@vetmed.uni-giessen.de)  
35 RPC: [rtpayan@uevora.pt](mailto:rtpayan@uevora.pt)  
36 SA: [selim.aslan@neu.edu.tr](mailto:selim.aslan@neu.edu.tr)  
37 IMR: [ireichler@vetclinics.uzh.ch](mailto:ireichler@vetclinics.uzh.ch)  
38 KR: [karine.reynaud@inrae.fr](mailto:karine.reynaud@inrae.fr)  
39 MPK: [kowalewski@vetanat.uzh.ch](mailto:kowalewski@vetanat.uzh.ch) or [kowalewski@yahoo.de](mailto:kowalewski@yahoo.de)  
40

41 **Running title**

42 HSD11B1 and -2 expression in the canine placenta  
43

44 **Summary Sentence**

45 The canine placenta appears to have increased trophoblast-mediated inactivation of cortisol  
46 during mid-pregnancy, whereas parturition appears to be marked by increased local cortisol  
47 availability.

48

49 **Keywords**

50 dog (*Canis lupus familiaris*), placenta, parturition, cortisol, hydroxysteroid 11-beta  
51 dehydrogenase (HSD11B) 1/2

52

53 **Abstract**

54 Apart from being stress mediators, glucocorticoids modulate the feto-maternal interface during  
55 the induction of parturition. In the dog, the prepartum rise of cortisol in the maternal circulation  
56 appears to be erratic, and information about its contribution to the prepartum luteolytic cascade  
57 is scarce. However, the local placental upregulation of glucocorticoid receptor (GR/NR3C1) at  
58 term led to the hypothesis that species-specific regulatory mechanisms might apply to the  
59 involvement of cortisol in canine parturition. Therefore, here, we assessed the canine  
60 uterine/utero-placental spatio-temporal expression of hydroxysteroid 11-beta dehydrogenase 1  
61 (HSD11B1; reduces cortisone to cortisol), and -2 (HSD11B2; oxidizes cortisol to the inactive  
62 cortisone). Both enzymes were detectable throughout pregnancy, their transcriptional levels  
63 were elevated following implantation, with a strong increase in *HSD11B2* post-implantation  
64 (days 18-25 of pregnancy), and in *HSD11B1* at mid-gestation (days 35-40) ( $P<0.05$ ).”.  
65 Interestingly, when compared pairwise, *HSD11B2* transcripts were higher during post-  
66 implantation, whereas *HSD11B1* dominated during mid-gestation and luteolysis ( $P<0.05$ ). A  
67 custom-made species-specific antibody generated against HSD11B2 confirmed its decreased  
68 expression at prepartum luteolysis. Moreover, in mid-pregnant dogs treated with aglepristone,  
69 *HSD11B1* was significantly higher than -2 ( $P<0.05$ ). HSD11B2 (protein and transcript) was  
70 localized mostly in the syncytiotrophoblast, whereas *HSD11B1* mRNA was mainly localized  
71 in cytotrophoblast cells. Finally, in a functional approach using placental microsomes, a  
72 reduced conversion capacity to deactivate cortisol into cortisone was observed during  
73 prepartum luteolysis, fitting well with the diminished HSD11B2 levels. In particular, the latter  
74 findings support the presence of local increased cortisol availability at term in the dog,  
75 contrasting with an enhanced inactivation of cortisol during early pregnancy.

76

77 **1. Introduction**

78 The adrenal-derived cortisol, besides its association with stress, is involved in biological  
79 processes including reproductive events such as fetal development and the parturition cascade  
80 [1, 2]. Parturition is an orchestrated, mostly species-specific event, involving complex

81 endocrine signaling cascades that are still not fully characterized in several eutherian species.  
82 The sheep is one of the animal species in which the initiation of parturition is well studied and  
83 serves as a translational model for other domestic animal species. Thus, in this animal model,  
84 parturition appears to be triggered by increased amounts of fetal adrenal-derived cortisol [1, 3],  
85 inducing a shift in placental steroidogenic activity towards increased estradiol (E2) production,  
86 replacing the local progesterone (P4) production. This leads to increased secretion of placental  
87 prostaglandin (PG) F<sub>2</sub> $\alpha$ , which stimulates myometrial activity [1, 3]. The luteolytic activity of  
88 cortisol-induced and placenta-derived PGF<sub>2</sub> $\alpha$  plays further important roles in species where the  
89 corpus luteum is, at least in part, the source of P4, e.g., pig, cow, goat, mouse, cat, and rabbit  
90 [4]. Interestingly, in guinea pigs, humans, and other primates, parturition occurs in the presence  
91 of high circulating amounts of P4, accompanied, however, by local, i.e., placental, withdrawal  
92 of P4 signaling [5-8]. Accordingly, several mechanisms, involving local metabolism,  
93 differential expression of P4 receptor (PGR) isoforms, synthesis and availability of lower  
94 activity P4 metabolites, and accessibility of transcription factors, have been implied in the  
95 underlying regulatory mechanisms [s. reviewed in 7, 9]. In addition, the competitive binding  
96 activity observed between the glucocorticoid receptor (GR/NR3C1) and PGR [10, 11] is also  
97 thought to contribute to the functional local withdrawal of P4 in human placenta [12]. In  
98 contrast, cortisol appears to have a low binding capacity to PGR at physiological levels [10,  
99 13].

100 The unique endocrinological features of the dog, when compared with other domestic  
101 mammals, hinder the translation of different parturition-associated biological strategies  
102 observed in other species. The dog is the only domestic mammal in which no steroidogenic  
103 activity is observed in the placenta, with P4 being produced solely by the corpus luteum (CL)  
104 [14, 15]. This further accounts for the absence of a parturition-specific increase of estrogens  
105 [14, 16]. Furthermore, due to the absence of anti-luteolytic mechanisms during early diestrus,  
106 the dog presents an inherently regulated and long lasting activity of the CL [17, 18]. In the  
107 canine endotheliochorial placenta, maternal stroma-derived decidual cells are the only cellular  
108 population expressing the nuclear PGR [19-21]. This distribution of PGR is especially  
109 important when considering the parturition cascade. The prepartum decline of circulating P4  
110 levels, or functional blocking of PGR with antigestagens (e.g., aglepristone), results in  
111 decreased decidual cell-mediated P4/PGR signaling, associated with increased prepartum  
112 production of luteolytic PGF<sub>2</sub> $\alpha$  by the trophoblast, and leading to parturition/abortion [22].

113 Regarding canine cortisol, increased circulating amounts have been reported in dogs at the time  
114 of parturition [14, 23-25]. However, due to wide variation in detected levels, ranging from nadir

115 to clearly measurable values, elevated circulating cortisol levels are not considered a  
116 prerequisite for the induction of parturition in dogs and could be indicative of maternal stress  
117 [14, 23]. Nevertheless, despite its weak clinical applicability (repeated treatments with high  
118 dosages over longer time, associated with strong side effects), the termination of canine  
119 pregnancy can be induced with exogenously-administered glucocorticoids during the last third  
120 of pregnancy [26-28]. Furthermore, GR/NR3C1 was detected in the canine fetal trophoblast,  
121 and was upregulated in the placenta at the time of prepartum luteolysis [29]. Interestingly, in  
122 samples collected after preterm induction of luteolysis with aglepristone, GR/NR3C1  
123 expression remained unaffected, despite the increased PGF $2\alpha$  output observed following  
124 treatment [21]. Jointly, these observations exclude the increased availability of GR/NR3C1 as  
125 a requirement for the prepartum release of PGF $2\alpha$  in the dog [29]. Instead, it was proposed that  
126 GR/NR3C1 could be involved in a P4 withdrawal mechanism [29], similar to its proposed role  
127 in humans [12].

128 Underlying the present project, we hypothesized that glucocorticoids might be involved in the  
129 parturition cascade in the dog, and that their signaling and availability might be regulated  
130 locally in the placenta. Accordingly, recently, changes in the placental transcriptional profile  
131 during parturition were investigated in canine placental samples collected during mid-  
132 pregnancy and at the time of luteolysis, both prepartum and antigestagen-induced (abortion at  
133 mid-term) [30]. Among the differentially expressed genes were factors identified as potentially  
134 modulated by P4, i.a., hydroxysteroid 11-beta dehydrogenase 2 (*HSD11B2*), that, although  
135 being initially abundantly expressed, was downregulated during the termination of pregnancy  
136 [30]. HSD11B2, together with HSD11B1, interconvert the biologically inactive cortisone and  
137 the active cortisol [31]. HSD11B1 is predominantly a reductase, reducing cortisone into  
138 cortisol, and is expressed in several tissues (e.g., liver, adipose tissue and placenta, central  
139 nervous system, cardiovascular system or immune system), where it increases the intracellular  
140 glucocorticoid availability [31, 32]. Moreover, HSD11B1 can act as a dehydrogenase under  
141 specific circumstances, mainly associated with the disruption of cellular activity and/or  
142 metabolic disturbances like diabetes or obesity [31, 32]. In contrast, HSD11B2 acts solely as a  
143 dehydrogenase, decreasing local cortisol availability by converting it into cortisone [31]. The  
144 cortisol-inactivating function of HSD11B2 in the placenta acts as a protective mechanism  
145 against the passage of glucocorticoids into fetal circulation in humans [33]. However, the only  
146 information to date about these factors in the canine placenta is from the transcriptomic study  
147 [30]. To contribute to the knowledge regarding local regulatory mechanisms, and test our  
148 hypothesis regarding the local involvement of cortisol metabolism in the maintenance of canine

149 pregnancy, we investigated the expression and regulation of HSD11B1 and -2 in the canine  
150 uterus and/or placenta throughout pregnancy.

151

## 152 **2. Materials and Methods**

### 153 **2.1 Tissue collection and preservation**

154 Uterine/utero-placental samples from 41 clinically healthy crossbred sexually mature bitches  
155 were collected by routine ovariohysterectomy. Several of these tissue samples originated from  
156 previous studies, where details on animal manipulation and staging of pregnancy are described  
157 [21, 30, 34-37]. Animal experiments were carried out in accordance with animal welfare ethical  
158 principles and legislation, and approved by the responsible ethics committees of the Justus-  
159 Liebig University Giessen, Germany (permits no. II 25.3-19c20- 15c GI 18/14 and VIG3-19c-  
160 20/ 15 GI 18,14); of the University of Ankara, Turkey (permits no. Ankara 2006/06 and 2008-  
161 25- 124); and of the national review board CNREEA #16 (APAFIS #2015042112442132) for  
162 the Alfort Veterinary School (facility 947-046-2), France. Further samples from animals  
163 submitted to routine ovariohysterectomy at the Section of Small Animal Reproduction,  
164 Vetsuisse Faculty, Zurich, were collected after the owners' informed consent.

165 The onset of spontaneous estrus was observed in all animals, with the day of ovulation being  
166 determined when circulating P4 concentration exceeded 5 ng/ml. After the required period for  
167 oocyte maturation in the oviduct, i.e., 2-3 days [17], animals were mated (day 0 of pregnancy).  
168 Uterine or utero-placental samples (depending on the pregnancy stage) were divided in the  
169 following groups: non-pregnant animals (E-, days 8 - 12 after mating, n = 5), pre-implantation  
170 (E+, days 8 - 12 of pregnancy, n = 5), time of implantation (Day 17, n = 4), post-implantation  
171 (Post-Imp, days 18 - 25 of pregnancy, n = 7), mid-gestation (Mid-Gest, days 35 - 40 of  
172 pregnancy, n = 6), prepartum luteolysis (Lut, n = 4), 24h after aglepristone treatment (Agle 24h,  
173 n = 5) and 72h after aglepristone treatment (Agle 72h, n = 5). As implantation takes place at  
174 day 17 [20, 38, 39], confirmation of pregnancy during early pre-implantation period was  
175 performed with embryo flushing (E+). Animals in which no embryos could be retrieved  
176 between days 8 - 12 were allocated to the non-pregnant control group (E-). Samples from the  
177 Lut group were collected during active prepartum P4 decline, determined by hormonal  
178 measurements every 6h until P4 concentrations were below 3 ng/ml in three consecutive  
179 assessments. Aglepristone (Alizine, Virbac, Bad Oldesloe, Germany) was used to induce the  
180 termination of pregnancy in 10 animals at mid-pregnancy (days 40 - 45 after mating), following  
181 the protocol provided by the supplier, i.e., administration of 10 mg/kg body weight twice 24h

182 apart. Samples containing uterine and placental sections were collected 24 or 72h after the  
183 second administration of aglepristone.

184 After surgery, samples were washed with PBS and dissected from connective tissue. Samples  
185 used for RNA and protein analysis were immersed in RNAlater (Ambion Biotechnology  
186 GmbH, Wiesbaden, Germany) at 4°C for 24h and then stored at -80°C until needed. For  
187 histology, samples were fixed in 10% phosphate-buffered formalin for 24h, washed with PBS  
188 for 7 consecutive days, dehydrated in an ethanol series, transferred into xylol and embedded in  
189 paraffin. Whereas all samples were used for TaqMan PCR, 3 samples/group were used for  
190 immunohistochemistry and *in situ* hybridization experiments.

191

## 192 **2.2 RNA isolation, reverse transcription and semi-quantitative real-time TaqMan PCR**

193 The isolation of total RNA was performed with TRIzol reagent (Invitrogen, Varlsbad, CA,  
194 USA), following the supplier's instructions. A NanoDrop 2000 spectrophotometer  
195 (ThermoFisher Scientific AG, Reinach, Switzerland) was used to assess RNA quantity and  
196 purity. For each sample, RNA was cleaned of possible contaminating genomic DNA with the  
197 RQ1 RNA-free DNase kit (Promega, Dübendorf, Switzerland), and reverse transcribed using  
198 the MultiScribe Reverse Transcriptase with random hexamers used as primers (Applied  
199 Biosystems by Thermo Fisher, Foster City, CA, USA); cDNA corresponding to 1.2µg of total  
200 RNA was used per sample and reaction. The relative gene expression was assessed by semi-  
201 quantitative real time TaqMan PCR, following the previously described protocol [40, 41], in  
202 an ABI PRISM 7500 Sequence Detection System fluorometer (Applied Biosystems). All  
203 reactions were run in duplicate with Fast Start Universal Probe Master (Roche Diagnostics AG,  
204 Basel, Switzerland) and gene expression TaqMan assays targeting *HSD11B1*  
205 (Cf02626817\_m1) and *HSD11B2* (Cf02690463\_s1), all obtained from Applied Biosystems.  
206 Autoclaved water and non-reverse transcribed DNase-treated RNA were used as negative  
207 controls. Relative quantification was performed with the comparative Ct method ( $\Delta\Delta Ct$ ),  
208 following logarithmic transformation of values, calibrated to the average expression among all  
209 samples, and normalized to the expression of reference genes. Initially, three reference genes  
210 were evaluated, following our recent description [42]: *PTK2* (Cf02684608\_m1), *EIF4H*  
211 (Cf02713640\_m1) and *KDM4A* (Cf02708629\_m1). The evaluation of the stability of the  
212 reference genes was further assessed with RefFinder [43]. Since *PTK2* and *KDM4A* were more  
213 stable than *EIF4H* in the samples used in this study, these two genes were used for the  $\Delta\Delta Ct$   
214 calculation.

215 For the compartmentalization studies, formalin-fixed and paraffin-embedded (FFPE) utero-  
216 placental samples from 3 animals belonging to Mid-Gest or Lut groups were used, according  
217 to our previously described protocol [29, 44]. A total of 3 tissue sections per animal were cut  
218 with 5 µm thickness and mounted on Arcturus PEN membrane glass slides (LCM0522, Applied  
219 Biosystems). Tissue sections were then deparaffinized, rehydrated, stained with hematoxylin  
220 for histological visualization and dried overnight at 37°C. Using a stereomicroscope, the  
221 different utero-placental compartments (i.e., placental labyrinth, endometrium and  
222 myometrium) were identified and dissected with sterile scalpel blades. Total RNA was isolated  
223 using the RNeasy FFPE Kit (Qiagen GmbH, Hilden, Germany), following the manufacturer's  
224 protocol, and RNA concentration was measured with a NanoDrop 2000. Following the variable,  
225 and sometimes low, yield of RNA obtained from these samples (ranging 43 to 416 ng/µl), 10  
226 ng of RNA were DNase treated and reverse transcribed with the High Capacity cDNA Reverse  
227 Transcription Kit (Applied Biosystems). Afterwards, the obtained cDNA was amplified with  
228 the TaqMan PreAmp Master Mix kit, following the supplier's protocols and as previously  
229 described [40]. For this, TaqMan assays for *HSD11B1*, *HSD11B2* and reference genes were  
230 pooled and mixed with the previously prepared cDNA and TaqMan Preamp Master Mix.  
231 Samples were then amplified using an Eppendorf Mastercycler (Vaudax-Eppendorf AG, Basel,  
232 Switzerland). Following this, the semi-quantitative PCR and relative gene expression  
233 quantification was performed as described above.

234

### 235 **2.3 Immunohistochemistry (IHC)**

236 Since no species-specific or cross-reacting antibodies were commercially available for the  
237 canine species, the development of polyclonal antibodies was attempted, as previously  
238 described [44], and was successful for generating a custom-made anti-HSD11B2 antibody (but  
239 not for HSD11B1) (Eurogentec Seraing, Belgium). Therefore, guinea pigs were immunized  
240 using the peptide sequence C+RALRPGQPGSTPAQ (aa 270-284) and  
241 C+LAAQPRRRYYPGRGL (aa226-240), based on the available sequences (GenBank  
242 accession number XM\_005620822.3). Cysteine (C+) was added to the N-terminal to allow  
243 peptide conjugation to carrier proteins, and the NH<sub>2</sub>-terminus was added to the C-end of the  
244 peptide to mimic the uncharged peptide bond in the protein. After preliminary assessments of  
245 IHC staining, the affinity purified antibody targeting the sequence C+RALRPGQPGSTPAQ  
246 was used in further analyses.

247 The standard indirect immunoperoxidase method was used for IHC to localize the expression  
248 of HSD11B2 protein in the canine placenta during post-implantation, mid-gestation and

249 prepartum luteolysis. Additionally, to allow for better differentiation between cell types,  
250 consecutively cut slides from mid-gestation animals were stained against the endothelin  
251 receptor B (goat polyclonal anti-EDNRB, sc-21196, Santa Cruz Biotechnology), staining for  
252 syncytiotrophoblast [45], and nuclear progesterone receptor (mouse monoclonal anti-PGR,  
253 IM1408, Beckman Coulter Life Sciences, Indianapolis, IN, USA), staining for decidual cells  
254 [21]. IHC was performed as previously described [40, 41]. Sections with 3 µm of FFPE tissue  
255 samples were mounted on microscope slides (SuperFrost; Menzel-Glaeser, Braunschweig,  
256 Germany), deparaffinized and rehydrated. Antigen retrieval was performed by heating in a  
257 microwave oven with Tris-EDTA buffer (10mM Tris base + 1mM EDTA solution, pH = 9, for  
258 HSD11B2) or 10mM citrate buffer (pH = 6, for PGR and EDNRB). After quenching  
259 endogenous peroxidase activity with 0.3% hydrogen peroxidase in methanol, slides were  
260 incubated in 10% goat or horse serum (depending on the secondary antibody) to decrease  
261 nonspecific binding, and then incubated overnight at 4°C with primary antibodies at the  
262 following dilutions: anti-HSD11B2 diluted at 1:1000; anti-PGR at 1:100.; EDNRB at 1:200.  
263 Pre-immune serum (in the case of HSD11B2) or non-immune IgG (in the case of PGR and  
264 EDNRB) were used as negative/isotype controls (goat IgG I-5000, and mouse IgG I-2000, both  
265 from Vector Laboratories Inc., Burlingame, CA, USA), at the same protein concentration as the  
266 primary antibodies. Following the incubation with a biotinylated secondary antibody diluted at  
267 1:100 (BA-7000 goat anti-guinea pig for HSD11B2; BA-9500 horse anti-goat IgG for EDNRB;  
268 BA-2000 horse anti-mouse IgG for PGR; all from Vector Laboratories Inc.) and with  
269 streptavidin-peroxidase ABC kit (Vector Laboratories Inc.), positive signals were revealed with  
270 the Liquid DAB+ substrate kit (Dako Schweiz AG, Baar, Switzerland). Slides were then  
271 counterstained with haematoxylin, dehydrated and mounted with Histokit (Assistant, Osterode,  
272 Germany). The localization of positive signals and capture of representative pictures were  
273 performed with a Leica DMRXE light microscope equipped with a Leica Flexacam C1 camera  
274 (Leica Microsystems, Wetzlar, Germany).

275

#### 276 **2.4 *In situ* hybridization (ISH)**

277 As the coding sequence available for canine *HSD11B2* in GenBank was only predicted,  
278 molecular cloning was performed to confirm the sequence and generate templates for cRNA to  
279 be used in ISH. Therefore, the following primers were used: forward: 5'-CCA AGA AGC TAG  
280 ATG CCA TG-3', reverse: 5'-CCT GTG GGC ACT GCT CAT T-3' (ordered from Microsynth  
281 AG, Balgach, Switzerland), generating amplicons of 937 bp. Hot start PCR was applied with  
282 AmpliTaq Gold DNA polymerase (Applied Biosystems) using two uterine cDNA samples;



283 annealing temperature was set at 58°C. PCR products were separated on a 2% agarose gel  
284 stained with ethidium bromide and isolated using the QIAquick Gel Extraction Kit (Qiagen  
285 GmbH). The products were then subcloned into pGEM-T vector (Promega) before  
286 transforming into XL1 Blue competent cells (Stratagene, La Jolla, CA, USA) for multiplication.  
287 Plasmids were isolated with the PureYield Plasmid Miniprep System (Promega), and control  
288 double-digestion was performed with NcoI and NotI restriction enzymes (New England  
289 Biolabs, Frankfurt, Germany). Plasmids were then sent for commercial sequencing (Microsynth  
290 AG). The partial sequence of canine-specific *HSD11B2* was submitted to GenBank with the  
291 accession number.

292 In the next step, the cellular localization of transcripts encoding for both enzymes was assessed  
293 with non-radioactive ISH, following our previously published protocols [21, 46, 47]. Placentae  
294 collected during mid-gestation and parturition luteolysis were used. In addition to the cloned  
295 sequence of *HSD11B2* that was used as a template for generating riboprobes, the canine-  
296 specific *HSD11B1* sequence was available in GenBank: NM\_001005756.1. The following  
297 primers were then used for both targets; *HSD11B1* for: 5'-GCA GAA GCA TGG AAG TCA  
298 AC-3', rev: 5'-TGA GGC CGA GGA TAC AGA G-3', 251 bp; and *HSD11B2* for: 5'- ACC  
299 TCA GCC CAG TCG TAG AT-3', rev: 5'- AGG GCC TTC ATT TGG ATC TGG -3', 248bp  
300 (ordered from Microsynth). The PCR products were then purified and subcloned into pGEM-T  
301 plasmids following the protocol described above. The specificity and identification of sense  
302 and anti-sense direction of products in the plasmid was performed by commercial sequencing  
303 of plasmids single cut with either NcoI or NotI restriction enzymes (Microsynth AG), and  
304 cRNA probes labelled with digoxigenin (DIG) were synthesized using the DIG-RNA Labelling  
305 Kit (Roche Diagnostics AG). The efficiency of riboprobes synthesis was confirmed with a dot-  
306 blot analysis, evaluating signal intensity in serial dilutions of the probes in positively charged  
307 nylon membranes stained against DIG (Roche Diagnostics AG). In the next step, tissue sections  
308 of 2 µm thickness were mounted on microscope slides, deparaffinized in xylene, rehydrated,  
309 digested with 70 µg/ml proteinase K for 19 mins at 37°C (Sigma-Aldrich Chemie GmbH) and  
310 post-fixed with 4% paraformaldehyde. *In situ* hybridization of cRNA probes was performed  
311 overnight at 37°C in the presence of formamide. Sense probes served as negative controls. After  
312 blocking of nonspecific signals with 3% ovine serum, samples were incubated overnight with  
313 alkaline phosphatase-conjugated sheep anti-DIG Fab Fragments diluted 1:5000 (Roche  
314 Diagnostics AG). Endogenous alkaline phosphatase signals were blocked with levamisole.  
315 Detection of positive signals was performed with 5-bromo-4-chloro-3-indolyl phosphate and  
316 nitroblue tetrazolium (BCIP/NBT, Roche Diagnostics AG). Representative pictures were

317 obtained with a Leica DMRXE light microscope equipped with a Leica Flexacam C1 camera  
318 (Leica Microsystems).

319

## 320 **2.5 Protein extraction and western blot**

321 The relative protein expression of HSD11B2 was assessed, following our previously published  
322 protocols [35, 48]. Randomly selected utero-placental samples from post-implantation, mid-  
323 gestation and parturition luteolysis groups (n = 3/group) were homogenized in lysis buffer (Net2  
324 Buffer: 50 mM Tris-HCl, pH = 7.4, 300 mM NaCl, 0.05% NP-40; containing 10µl/ml of  
325 protease inhibitor cocktail) on using an IKA Euro-ST D overhead stirrer (IKA-Werke GmbH,  
326 Staufen, Germany). Samples were then centrifuged (10 min at 10,000 g) and the protein content  
327 of the supernatants was then quantified with the Bradford assay using a SmartSpec Plus  
328 spectrophotometer (Bio-Rad Laboratories, Munich, Germany). Protein samples were  
329 normalized with a sample buffer (25 mM Tris-Cl, pH = 6.8, containing 1% SDS, 5% β-  
330 mercaptoethanol, 10% glycerol and 0.01% bromophenol blue), and 20 µg of protein from each  
331 sample were heated at 95°C for 10 min, followed by electrophoresis separation in a 10%  
332 polyacrylamide gel (AppliChem GmbH, Darmstadt, Germany). Proteins were then transferred  
333 into a methanol-activated polyvinylidene difluoride (PVDF) membrane (Bio-Rad  
334 Laboratories). Non-specific binding sites were blocked with 5% low-fat powdered milk diluted  
335 in PBST (PBS + 0.25% Tween-20), and membranes were incubated overnight at 4°C with anti-  
336 HSD11B2 antibody diluted at 1:250 in 2.5% low-fat powdered milk in PBST solution.  
337 Membranes were then incubated with a rabbit anti-guinea pig horseradish peroxidase (HRP)-  
338 conjugated antibody (1: 15000, A5545, Sigma Aldrich Chemie GmbH, Buchs, Switzerland),  
339 followed by the detection of signals with the SuperSignalWest Chemiluminescent Kit substrate  
340 (Thermo Fisher Scientific AG, Reinach, Switzerland) in a Chemi-Doc XRS+ System and Image  
341 Lab Software (Bio-Rad Laboratories). To ensure specificity, anti-HSD11B2 antibody was  
342 incubated for 1h at ambient temperature with the immunization peptide (blocking peptide) at  
343 the same dilution, before being used to blot the membrane. For loading control and relative  
344 quantification, PVDF membranes were re-blotted with mouse monoclonal antibody against  
345 ACTINB (1:1000, sc-69879, Santa Cruz Biotechnology, Santa Cruz, CA, USA), followed by a  
346 goat anti-mouse HRP-labelled secondary antibody (1: 15000, W402B, Promega). The optical  
347 density of bands was measured with ImageJ software (US National Institutes of Health,  
348 Bethesda, Maryland, USA). Relative protein expression was calculated by normalizing the  
349 optical density of HSD11B2 against ACTINB in the reblotted membranes and is presented as  
350 standardized optical density (SOD).

351

## 352 **2.6 Evaluation of uteroplacental cortisol-cortisone conversion capacity**

353 To evaluate the capacity of placental tissue to interconvert cortisol and cortisone, microsomal  
354 fractions (crude endoplasmic reticulum) were isolated from utero-placental sections collected  
355 during the post-implantation period, as well as from placenta and endometrium, and myometrial  
356 samples (macroscopically dissected) at the time of prepartum luteolysis (n = 4/group). This was  
357 done using the Endoplasmic Reticulum Isolation Kit (Sigma Aldrich Chemie GmbH),  
358 according to the manufacturer's directions and as previously described [49].

359 All conversion capacity assays were performed blinded, using incubation protocols modified  
360 after [49, 50]. Reaction mixtures (100  $\mu$ l volume) were created by combining 50  $\mu$ l of  
361 microsomal fractions with co-factors and substrates. For the cortisol to cortisone conversion  
362 assay, 0.25 mM NAD<sup>+</sup> (Roche Diagnostics, Mannheim, Germany) was used as co-factor, and  
363 substrate was 25 nM of unlabeled cortisol (Merk KGaA, Darmstadt, Germany) and 1.82 nM  
364 (20 000 cpm) of tritium-labeled [1,2,6,7-<sup>3</sup>H(N)]-cortisol (PerkinElmer LAS GmbH, Rodgau,  
365 Germany). For the cortisone to cortisol conversion assay, the co-factor was 0.25 mM NADPH  
366 +H<sup>+</sup> (Roche Diagnostics), while the substrates were 25 nM of unlabeled cortisone (Merk  
367 KGaA) and 7.5 nM (60 000 cpm) of tritium-labeled [1,2-<sup>3</sup>H(N)]-cortisone (PerkinElmer LAS  
368 GmbH). The use of a mixture of unlabeled and <sup>3</sup>H-labeled substrates was performed to  
369 minimize radioactive waste, while still allowing the evaluation of conversion rates. Mixtures  
370 using random samples were initially incubated for 0, 5, 10, 20 and 30 mins at 37°C to determine  
371 the ideal incubation time. An incubation time of 20 mins was considered the most suitable time  
372 by showing the maximal conversion capacity of the mixture, and was then used for all  
373 subsequent experiments. After incubation was complete, samples were extracted with ethyl  
374 acetate, dried in a MicroDancer infrared vortex-evaporator (Hettich AG, Baech, Switzerland)  
375 and redissolved in 100  $\mu$ l of HPLC mobile phase (methanol/acetonitrile/water 43:3:54 v/v/v).  
376 Samples were then separated via HPLC, following the protocol described in [51]. In short, 20  
377  $\mu$ l of dissolved extracts were separated on a 150  $\times$  4 mm Eurospher II 100-5 C18 reversed-phase  
378 column in a Smartline Manager 5050 and Pump 150 HPLC system (all HPLC equipment from  
379 Knauer, Berlin, Germany) at a flow rate of 1 mL/min. Eluted fractions with 0.5 ml were then  
380 collected and evaporated. The <sup>3</sup>H-activity in HPLC fractions was then measure by adding the  
381 scintillation cocktail Rotiszint eco plus (Carl Roth GmbH, Karlsruhe, Germany) in a Tri-Carb  
382 2810 TR  $\beta$ -scintillation counter (PerkinElmer LAS GmbH). Differentiation between substrate  
383 and metabolite was based on a comparison of retention times with authentic tritiated standards.  
384 The percent of substrate conversion was calculated from the distribution of <sup>3</sup>H activity among

385 the peaks after subtracting technical background of  $\beta$ -scintillation counter and baseline  
386 correction.

387

## 388 **2.7 Statistical analysis**

389 Statistical evaluation of changes in relative transcript levels (relative gene expression, RGE)  
390 and protein amounts (standardized optic density, SOD) between different stages of pregnancy  
391 was performed by one-way ANOVA, followed by Tukey-Kramer multiple comparisons post-  
392 test. In addition, two-tailed unpaired Student's t-test was performed to evaluate possible  
393 differences in pairwise comparisons, i.e. between mRNA amounts of *HSD11B1* and -2 in  
394 different groups. The software GraphPad 2.06 (GraphPad Software Inc, San Diego, CA, USA)  
395 was used for this analysis and  $P < 0.05$  was considered as statistically significant.

396

## 397 **3. Results**

### 398 **3.1 Uterine/utero-placental gene expression during pregnancy**

399 The transcriptional availability of *HSD11B1* and -2 was evaluated in all uterine/utero-placental  
400 tissue samples. The mRNA availability of *HSD11B1* was significantly higher at mid-gestation,  
401 when compared with all earlier stages of pregnancy, and non-pregnant (E-) uterine samples ( $P$   
402  $< 0.001$ , Fig. 1A). There was a high variation in *HSD11B1* expression during luteolysis,  
403 yielding no significant difference between mid-gestation and luteolysis ( $P > 0.05$ , Fig. 1A).  
404 Yet, in antigestagen-induced luteolysis/abortion, the expression of *HSD11B1* was significantly  
405 increased 24 h after mid-pregnant animals were treated with aglepristone ( $P < 0.05$ , Fig. 1B).  
406 The availability of *HSD11B2* mRNA was the highest in post-implantation and mid-gestation  
407 samples, when compared with all other evaluated stages ( $P < 0.05$ , Fig. 1C). In contrast with  
408 *HSD11B1*, the expression of *HSD11B2* was downregulated in samples collected 24 and 72 h  
409 after aglepristone treatment ( $P < 0.05$ , Fig. 1D), resembling the pattern observed during normal  
410 luteolysis. In a pairwise comparison of both enzymes in canine uterine and utero-placental  
411 samples, *HSD11B2* expression was significantly higher than -1 during post-implantation ( $P <$   
412  $0.001$ , Fig. 1E). This changed during mid-gestation and prepartum luteolysis, with *HSD11B1*  
413 transcripts being more abundant than *HSD11B2* ( $P < 0.01$  and  $P < 0.05$ , respectively, Fig. 1E).  
414 A higher expression of *HSD11B1* than *HSD11B2* was further observed in animals treated with  
415 aglepristone ( $P < 0.01$ , Fig. 1F).

416

### 417 **3.2 Compartmentalization of *HSD11B1* and -2 mRNA in the canine uterus**

418 The mRNA abundance of all factors in different tissue layers, i.e., placental labyrinth,  
419 endometrium or myometrium, was assessed in utero-placental units collected during mid-  
420 gestation (i.e., in the mature fully developed placenta) and prepartum luteolysis. The  
421 availability of both *HSD11B1* and *HSD11B2* transcripts was frequently below detection limits  
422 in the myometrium of animals at mid-gestation resulting in the exclusion of these samples from  
423 the statistical evaluation. (Fig. 2). Due to high individual variability, no significant differences  
424 were observed for the expression of *HSD11B1* between the tissue compartments at mid-  
425 gestation ( $P > 0.05$ ). This contrasted with its expression during prepartum luteolysis, with the  
426 placenta showing significantly higher levels than endometrium or myometrium ( $P < 0.05$ , Fig.  
427 2A), suggesting the placenta as being the major source. *HSD11B2* transcripts were significantly  
428 more abundant in the mid-gestation placenta compared with mid-gestation endometrium ( $P <$   
429  $0.01$ ), and with the placental labyrinth and myometrium of prepartum luteolysis ( $P < 0.001$  and  
430  $P < 0.01$ , respectively, Fig. 2B). Furthermore, endometrial availability of *HSD11B2* was  
431 significantly higher than in the placenta during prepartum luteolysis ( $P < 0.05$ , Fig. 2B).

432

### 433 **3.3 Protein expression of HSD11B2 in the canine utero-placental unit**

434 The canine-specific anti-HSD11B2 antibody allowed the detection of a band close to the  
435 predicted protein size (44kDa) in western blot analysis (Fig. 3A). The signal was quenched with  
436 antibody pre-incubated with the immunization peptide (Fig. 3A). In utero-placental  
437 homogenates, HSD11B2 protein expression was significantly higher at post-implantation than  
438 mid-gestation and prepartum luteolysis ( $P < 0.01$  and  $P < 0.001$ , respectively, Fig. 3B),  
439 mirroring the time-dependent changes observed at the mRNA level.

440

### 441 **3.4 Localization of HSD11B1 and HSD11B2 in the canine placenta**

442 The availability of custom-made anti-HSD11B2 antibody has made it possible to study its  
443 expression at both the protein and RNA level, whereas the localization of HSD11B1 was  
444 possible only by applying ISH.

445 During post-implantation, HSD11B2 was predominantly localized at the embryo-maternal  
446 interface of the developing placenta, in invading cytotrophoblast cells (Fig. 4A, left panels). In  
447 the mature placenta, during mid-gestation, signals were mostly localized in the  
448 syncytiotrophoblast, with some weaker staining in other cellular components (e.g. decidual  
449 cells or endothelial cells (Fig. 4A, center panels)). At prepartum luteolysis, the signals were  
450 weaker and a more diffuse staining pattern was observed (Fig. 4A, right panels). The

451 localization of HSD11B2-positive signals in the syncytiotrophoblast was then confirmed in the  
452 mature placenta by performing staining of consecutive slides (Fig. 4B) against PGR, as a  
453 marker of decidual cells [19, 20], and EDNRB, expressed by the syncytiotrophoblast [45].  
454 With ISH, positive signals for *HSD11B1* were mostly localized in cytotrophoblast cells, with  
455 some signals also observed in maternal endothelial cells (Fig. 5A), while for *HSD11B2*, the  
456 signals were mainly observed in the syncytiotrophoblast, with a more diffuse pattern observed  
457 during luteolysis than during mid-gestation, as seen with IHC (Fig. 5B).

458

### 459 **3.5 Enzymatic conversion between cortisol and cortisone in canine placental homogenates**

460 The potential of the placenta to interconvert cortisol and cortisone was evaluated in samples  
461 collected during post-implantation, where a significantly higher mRNA availability of  
462 *HSD11B2* than *-1* was observed, and at the time of parturition luteolysis, where an inverted  
463 pattern, associated with decreased protein expression of HSD11B2, was observed. Due to  
464 difficulties in the separation of intact tissue layers containing the invading trophoblast from  
465 remaining tissue layers in the still developing utero-placental interface at post-implantation, full  
466 tissue cross-sections were used for post-implantation specimens. On the other hand, in the fully  
467 developed placenta at parturition luteolysis, the separation between physiological layers of  
468 placenta with adjacent endometrium from myometrium (the latter presenting low mRNA  
469 availability of both factors, being used as a negative control) was performed at the level of  
470 physiologically significantly enlarged endometrial chambers (i.e., deep endometrial glands).  
471 When evaluating conversion rates, values below 5% were considered as unreliable, as the  
472 presence of impurities or decay of the cortisol tracer, in addition to possible technical  
473 background of the beta counter, can mask weak conversion effects.

474 The conversion of cortisol into cortisone (i.e., inactivation of cortisol, indicating HSD11B2  
475 activity), was significantly higher in utero-placental samples collected at post-implantation,  
476 when compared with the conversion rate observed with microsomes isolated from either the  
477 placenta or myometrium obtained during parturition luteolysis ( $P < 0.05$ , Fig. 6). In contrast,  
478 the conversion of cortisone into cortisol (i.e., activation of cortisol) was undetected in post-  
479 implantation samples and myometrium from luteolysis, or remained below 1% in placental +  
480 endometrium samples collected during luteolysis (not shown).

## 481 **4. Discussion**

482 In the attempt to gain new insights into the utero-placental availability of cortisol in the dog,  
483 we evaluated the expression and localization of cortisol-to-cortisone interconverting enzymes

484 HSD11B1 and -2 in the canine uterus and utero-placental compartments throughout pregnancy.  
485 Both cortisol-regulating enzymes were expressed in all samples. Based on their significantly  
486 lower uterine expression at the pre-implantation stage (E+) and in corresponding non-pregnant  
487 controls (E-), as well as on the day of implantation (day 17), than in later gestational stages,  
488 they appeared to be predominantly associated with placental development and functionality.  
489 Therefore, subsequent analyses focused mainly on stages of pregnancy in which a placenta was  
490 present, i.e., post-implantation, mid-gestation and prepartum luteolysis. Indeed, *in situ*  
491 hybridization analysis of both factors, and immunohistochemical detection of HSD11B2,  
492 localized both enzymes predominantly to the fetal-derived trophoblast cells within the canine  
493 placental labyrinth.

494 The transcriptional availability of *HSD11B1* was the highest at mid-gestation, while *HSD11B2*  
495 mRNA levels were already increased during post-implantation. Therefore, there seemed to be  
496 a higher transcriptional availability of *HSD11B2* than *HSD11B1* associated with early  
497 placentation (post-implantation). An excessive exposure to glucocorticoids can cause  
498 detrimental effects in the establishment of pregnancy and in fetal development in different  
499 species [33, 52, 53]. Several of these effects are associated with disrupted expression of  
500 HSD11B2 [54, 55]. Thus, the cortisol-inactivating capacity of HSD11B2 has been  
501 characterized as a protective barrier against the passage of glucocorticoids into fetal circulation  
502 [33, 56-58]. In humans, e.g., fetal glucocorticoids are 5-10 times lower than maternal  
503 circulatory levels [59]. Although several studies have attempted to measure fetal exposition to  
504 cortisol in the dog using, e.g., puppy hair and claws [60, 61], a clear comparison with maternal  
505 levels is still not available. Nevertheless, it appears plausible that such a protective mechanism  
506 might be present in the dog, too. This hypothesis appears to be further supported by the  
507 microsomes activity assay, where an increased conversion of cortisol into cortisone was  
508 observed in post-implantation samples when compared with luteolysis. With regard to the post-  
509 implantation group, the high variability might be due to individual variations or to time-  
510 dependent changes. Nevertheless, there is a clearly higher capacity for cortisol inactivation  
511 (conversion to cortisone) during post-implantation than at the prepartum luteolysis. Within the  
512 fully developed fetal placental compartment, the strongest HSD11B2-positive signals were  
513 mainly localized in the syncytiotrophoblast. A similar localization pattern was previously  
514 described in mice, with placental HSD11B2 being mainly associated with the trophoblast [62],  
515 as well as in humans, where it was exclusively detected in the syncytiotrophoblast [58, 63].  
516 Interestingly, in sheep, representing a non-invasive type of placentation, *HSD11B2* could be  
517 detected reliably in the trophoblast and endoderm of the conceptus, but not in the uterus,

518 during early pregnancy [64]. Thus, despite the weak signals observed in endothelial and  
519 decidual cells in the present study, the increased cortisol-deactivation, possibly associated with  
520 a protective embryonal mechanism against maternal cortisol, appears to be mainly mediated by  
521 the trophoblast during early fetal development.

522 The progression of pregnancy towards parturition was associated with a decreased utero-  
523 placental expression of HSD11B2, which was confirmed at both the mRNA and protein levels.  
524 This was also reflected in its low activity at prepartum luteolysis based on the microsomal  
525 cortisol conversion rates. In fact, with average conversions of 2% in the placenta and  
526 endometrium, and 1.9% in myometrium (both below the defined 5% threshold), luteolysis  
527 appears to be virtually devoid of cortisol into cortisone conversion activity. The decreased  
528 placental availability of HSD11B2 at term was also highlighted by the assessment of mRNA in  
529 different utero-placental compartments, showing its significantly lowered levels between fully  
530 developed mid-term placenta and prepartum luteolysis. Fitting with these observations was the  
531 lowered *HSD11B2* transcription in antigestagen-treated dogs, emphasizing the P4-dependent  
532 expression of HSD11B2. This supports our previous report using the transcriptomic approach  
533 [30], where *HSD11B2* was described as a downstream factor from P4 signaling. As several  
534 samples used in the present work derived from previous projects, serum samples that could  
535 allow a correlation between placental expression of HSD11B1/2 and circulating cortisol or P4  
536 were not available. Nevertheless, circulating P4 levels are described to a greater extent in the  
537 dog [s. reviewed in 65]. Thus, the time-dependent decrease of HSD11B2 expression appears to  
538 accompany, at least in part, the decreasing P4 circulating levels observed in this species,  
539 including the steep prepartum decline. In ovariectomized mouse, the uterine expression of  
540 *HSD11B2* could be upregulated by P4 administration, and later ablated by the PGR blocker  
541 mifepristone (RU486) [57]. Aglepristone used in our studies is a derivate of mifepristone, both  
542 type II antigestagens, with similarities in its chemical structure and activities related to the PGR  
543 [66]. Cumulatively, the recently postulated association between P4/PGR signaling and  
544 placental *HSD11B2* expression in the dog [30], is substantiated by the present findings, clearly  
545 indicating its importance in the luteolytic cascade.

546 The diffuse staining of HSD11B2 in the prepartum labyrinth could possibly be associated with  
547 its significantly lowered abundance and/or degradation. Conversely, the utero-placental  
548 availability of *HSD11B1* increased from post-implantation to mid-gestation, and remained  
549 unaffected at prepartum luteolysis. This was associated with an apparent shift in the  
550 transcriptional availability of both isoforms, with *HSD11B1* being significantly higher than -2  
551 at term. The ISH allowed the detection of mRNA encoding for *HSD11B1* mainly in the



552 cytotrophoblast, with some signals also identified in maternal endothelial cells during  
553 prepartum luteolysis. These observations suggest that a possible interplay between the cortisol-  
554 deactivating syncytiotrophoblast and cortisol-activating cytotrophoblast could be present in the  
555 canine placenta. For instance, in mice, increased expression of *HSD11B1* can be observed in  
556 late pregnancy in fetal tissue [62], and in humans it is localized in endothelial cells and different  
557 trophoblast populations, but not in the syncytiotrophoblast [67]. As part of the approach  
558 involving microsomal activities, we investigated the potential of the placenta to activate  
559 cortisol, thereby addressing the activity of HSD11B1, which was below reliable detection limits  
560 in the placenta from prepartum luteolysis, and was undetectable in myometrium and in post-  
561 implantation samples. The inclusion of a positive control tissue, which was not possible in this  
562 study, could provide a more definitive answer regarding the lack of cortisol activation. While  
563 the low detection of HSD11B1 activity, and the limitations in protein detection, could be  
564 explained by a low availability of this enzyme in the canine placenta, this remains to be  
565 confirmed. The higher utero-placental transcriptional availability of *HSD11B1* in the  
566 antigestagen treated dogs differed from that observed during normal parturition. A possible  
567 explanation could be in the local stress-related response to acute PGR withdrawal [s. reviewed  
568 in 66]. Despite the still veiled importance of the parturition-associated increase of cortisol  
569 activity in the dog, as mentioned elsewhere, the cortisol-stimulated shift in placental  
570 steroidogenesis described for other species [1, 3], does not apply to the dog [14, 15].  
571 Furthermore, only term, and not aglepristone-induced termination of pregnancy, was associated  
572 with the upregulation of GR/NR3C1 [29]. Nevertheless, the lower HSD11B2 activity appears  
573 to be associated with a locally increased availability of cortisol, possibly embryo-derived. This  
574 local cortisol increase could be an important event in the final maturation of the fetus,  
575 associated, e.g., with the final maturation of fetal organs, like the lung [68]. Still, the  
576 confirmation of such local events is still required, as previous cortisol measurements in the dog  
577 were performed at the circulating level [14, 23-25]. Furthermore, as already stated, termination  
578 of pregnancy in the dog is associated with increased circulating PGF2 $\alpha$  levels, deriving from  
579 the trophoblast and involving the 9-keto PGE2 reductase (9KPGR)-mediated synthesis from  
580 PGE2 [49]. An interplay between PGF2 $\alpha$  and cortisol has been described in several instances  
581 [1, 4]. However, the extent to which cortisol directly contributes to the placental PGF2 $\alpha$  output  
582 affecting the synthetic cascade of prostaglandins in the dog, including the rising COX2/PTGS2  
583 activity [21], remains to be investigated.

## 584 **5. Conclusions**

585 The results from the present work describe, for the first time, the presence of stage-dependent  
586 cortisol-modulating mechanisms in the canine placenta, mainly associated with the trophoblast.  
587 The higher expression of HSD11B2 in early placentation, associated with the local tissue  
588 potential to inactivate cortisol, might be involved in protective mechanisms of the embryo  
589 against maternal-derived glucocorticoids. The P4-dependent regulation of HSD11B2 is further  
590 substantiated by observation both during normal and induced parturition/abortion. A clear shift  
591 in placental regulation of cortisol activity is apparent at term, with parturition being associated  
592 with an increased *HSD11B1* mRNA availability, and decreased HSD11B2 expression and  
593 cortisol-inactivating activity. An interplay between different trophoblast populations is also  
594 apparent, with HSD11B1 being mainly localized in the cytotrophoblast, where GR/NR3C1 is  
595 also expressed [29], while HSD11B2-positive signals were mainly observed in the  
596 syncytiotrophoblast. Although its definitive role remains still to be defined for the dog, in  
597 accordance with our hypothesis, local cortisol appears to be involved in the termination of  
598 canine pregnancy and deserves more attention in the future.

## 599 **Conflict of interests**

600 The authors declare that they have no conflicts of interest.

601

## 602 **Author's contributions**

603 MTP was involved in developing the concept of the present study, experimental design,  
604 generating data, analysis and interpretation of data and drafting of the manuscript. GS was  
605 involved in the generation, analysis and interpretation of data, and revision of the manuscript.  
606 SA, RPC, IMR and KR were involved in the collection of tissue material, knowledge transfer,  
607 critical discussion and interpretation of data, and revision of the manuscript. MPK designed and  
608 supervised the project, was involved in interpretation of the data, and drafting and revision of  
609 the manuscript. All authors read and approved the final manuscript.

## 610 **Acknowledgements**

611 Authors are thankful to Dr. Sharon Mortimer for the careful editing of the manuscript. The  
612 technical expertise and contributions of Ricardo Fernandez Rubia and Kirstin Skaar are greatly  
613 appreciated. Part of the laboratory work was performed using the logistics at the Center for  
614 Clinical Studies, Vetsuisse Faculty, University of Zurich.

615

616 **Figure legends**

617 **Figure 1. Relative gene expression of HSD11B1 and HSD11B2 in the canine uterus/utero-**  
618 **placental compartment during pregnancy and in response to antigestagens.**

619 Relative gene expression is presented as determined by semi-quantitative real time (TaqMan)  
620 PCR ( $\bar{X}$  +/- SD). (A-D) To evaluate the effects of pregnancy progression, or of preterm  
621 termination of pregnancy with aglepristone, one-way non-parametric ANOVA was applied,  
622 revealing: (A)  $P < 0.0001$ , (B)  $P = 0.0197$ , (C)  $P < 0.0001$  and (D)  $P = 0.0009$ . When  $P < 0.05$ ,  
623 analysis was followed by a Tukey-Kramer multiple comparison post-test. (E, F) Comparison  
624 of relative gene expression between *HSD11B1* and *HSD11B2* at each stage was evaluated by  
625 applying Student's unpaired two-tailed t- test. Bars with asterisks differ at: \*  $P < 0.05$ , \*\*  $P <$   
626  $0.01$ , \*\*\*  $P < 0.001$ . E- = embryo-negative/non-pregnant animals, E+ = embryo-positive/pre-  
627 implantation, day 17 = time of implantation, Post-Imp = post-implantation, Mid-Gest = mid-  
628 gestation.

629

630 **Figure 2. Compartmentalization of HSD11B1 and HSD11B2 relative mRNA levels in the**  
631 **utero-placental tissue during mid-gestation and prepartum luteolysis.** Relative gene

632 expression, presented as  $\bar{X}$  +/- SD, was determined by semi-quantitative real time (TaqMan)  
633 PCR. Samples from 3 animals for each pregnancy stage were used. Differences between all  
634 groups was assessed with one-way non-parametric ANOVA, with  $P = 0.0079$  for HSD11B1  
635 and  $P < 0.0001$  for HSD11B2, followed by a Tukey-Kramer multiple comparison post-test. As  
636 the expression of both factors was frequently below detection limits in myometrium during  
637 mid-gestation, these samples were removed from statistical analysis. Bars with asterisks differ  
638 at: \*  $P < 0.05$ , \*\*  $P < 0.01$ , \*\*\*  $P < 0.001$ .

639

640 **Figure 3. Protein expression of HSD11B2 in utero-placental homogenates. (A)** Epitope-

641 blocking peptide was used to block HSD11B2-specific signal (~44kDa) in protein extract of  
642 utero-placental homogenates. (B) Representative immunoblots for HSD11B2 and ACTINB are  
643 shown. Standardized optical density (SOD) of HSD11B2 signals was measured in proteins  
644 extracted from utero-placental samples collected during post-implantation (Post-Imp), mid-  
645 gestation (Mid-Gest) and prepartum luteolysis. After quantifying HSD11B2 signals,  
646 membranes were re-blotted targeting ACTINB for normalization of signals intensity. SOD are  
647 presented as  $\bar{X}$  +/- SD. One-way non-parametric ANOVA revealed  $p = 0.0005$ , followed by a  
648 Tukey-Kramer multiple comparison post-test.

649

650 **Figure 4. Immunohistochemical localization of HSD11B2 in the canine placental labyrinth**  
651 **at selected stages of pregnancy. (A)** During post-implantation, signals were observed in the  
652 invading trophoblast. In the mature mid-gestation placenta, strong positive signals were  
653 localized in syncytiotrophoblast cells, with weak signals also being observed in other placental  
654 cell populations (e.g. endothelial and decidual cells). Samples collected at the time of parturition  
655 luteolysis appear to present a weaker and more diffuse pattern of staining. **(B)** The localization  
656 of HSD11B2-positive signals in the syncytiotrophoblast of the matured placenta was confirmed  
657 by performing consecutive staining of mid-gestation samples targeting PGR (expressed by  
658 decidual cells) and ETB (expressed by syncytiotrophoblast cells). No staining was observed in  
659 the isotype controls (insets in pictures, at the same magnification). Solid arrow = decidual cell;  
660 open arrow = endothelial cell; closed arrowhead = cytotrophoblast; open arrowhead =  
661 syncytiotrophoblast; asterisk = fetal stroma.

662  
663 **Figure 5. Localization of *HSD11B1* and *HSD11B2* mRNA in the canine placental**  
664 **labyrinth at mid-gestation and parturition luteolysis. (A)** *HSD11B1*-positive signals were  
665 mainly localized in cytotrophoblast and endothelial cells. Signal intensity in endothelial cells  
666 appeared to be stronger at parturition luteolysis than at mid-gestation. **(B)** *HSD11B2* was mainly  
667 expressed in the syncytiotrophoblast during mid-gestation, with a more diffuse pattern being  
668 observed at the time of parturition luteolysis. No staining was observed in the negative controls  
669 (sense probe; insets in pictures, at the same magnification). Open arrow = endothelial cell;  
670 closed arrowhead = cytotrophoblast; open arrowhead = syncytiotrophoblast.

671  
672 **Figure 6. Interconversion rate between cortisol and cortisone performed by canine utero-**  
673 **placental microsomes isolated from different stages of pregnancy.** Microsome conversion  
674 rates of cortisol into cortisone are presented as a percentage. Differences between groups was  
675 assessed with one-way non-parametric ANOVA ( $P = 0.0186$ ), followed by a Tukey-Kramer  
676 multiple comparison post-test. Bars with asterisks differ at: \*  $P < 0.05$ .

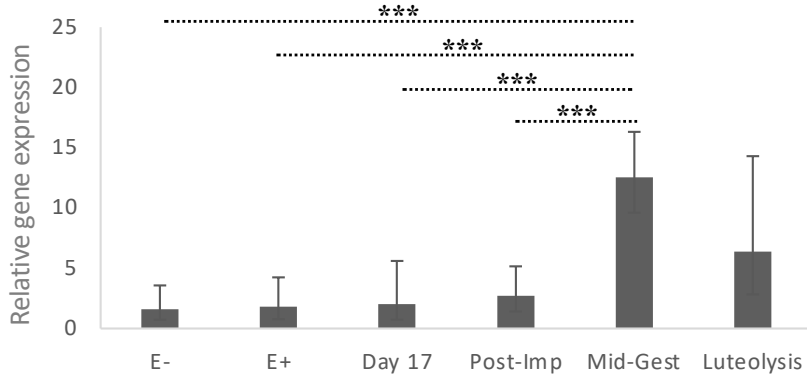
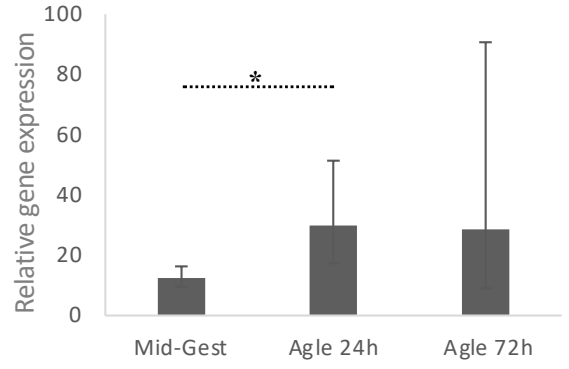
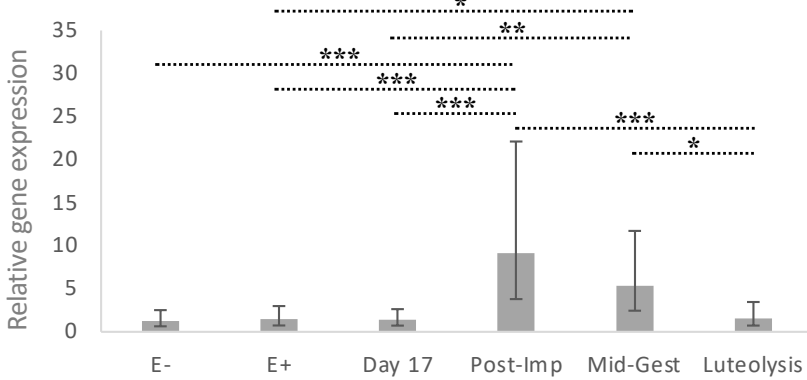
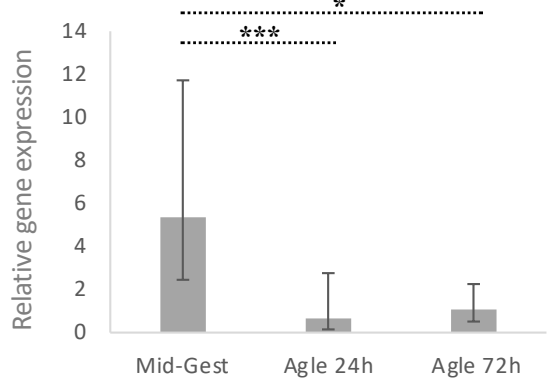
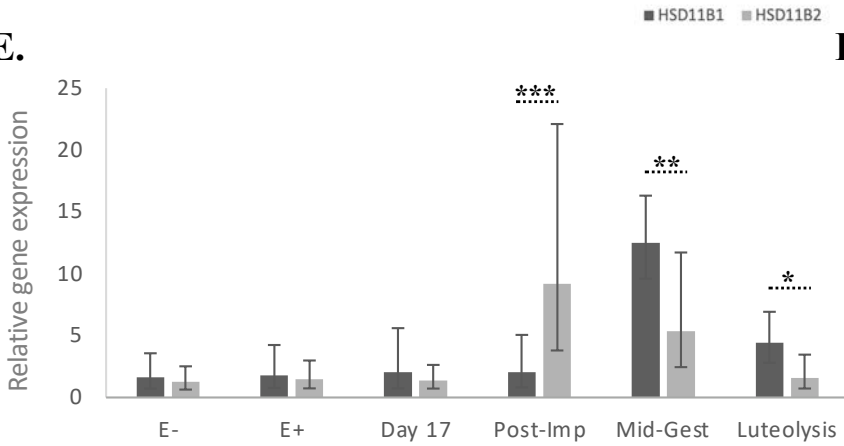
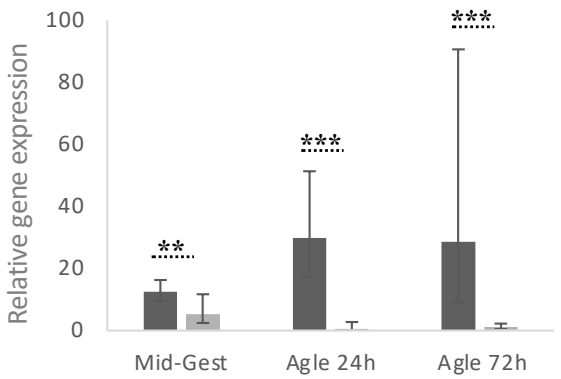
677  
678 **5. References**

- 679 1. Whittle, W.L., et al., *Glucocorticoid regulation of human and ovine parturition: the relationship between fetal*  
680 *hypothalamic-pituitary-adrenal axis activation and intrauterine prostaglandin production.* Biol Reprod, 2001. **64**(4):  
681 p. 1019-32.
- 682 2. Cottrell, E.C. and J.R. Seckl, *Prenatal stress, glucocorticoids and the programming of adult disease.* Front Behav  
683 Neurosci, 2009. **3**: p. 19.
- 684 3. Liggins, G.C., et al., *The mechanism of initiation of parturition in the ewe.* Recent Prog Horm Res, 1973. **29**: p. 111-  
685 59.
- 686 4. Schuler, G., R. Fürbass, and K. Klisch, *Placental contribution to the endocrinology of gestation and parturition.*  
687 *Animal Reproduction*, 2018. **15**(Suppl. 1): p. 822-842.

- 688 5. Tulchinsky, D., et al., *Plasma estrone, estradiol, estriol, progesterone, and 17-hydroxyprogesterone in human*  
689 *pregnancy. I. Normal pregnancy.* Am J Obstet Gynecol, 1972. **112**(8): p. 1095-100.
- 690 6. Heap, R.B. and R. Deanesly, *Progesterone in systemic blood and placenta of intact and ovariectomized pregnant*  
691 *guinea-pigs.* J Endocrinol, 1966. **34**(4): p. 417-23.
- 692 7. Mitchell, B.F. and M.J. Taggart, *Are animal models relevant to key aspects of human parturition?* Am J Physiol Regul  
693 Integr Comp Physiol, 2009. **297**(3): p. R525-45.
- 694 8. Nnamani, M.C., et al., *Evidence for independent evolution of functional progesterone withdrawal in primates and*  
695 *guinea pigs.* Evol Med Public Health, 2013. **2013**(1): p. 273-88.
- 696 9. Zakar, T. and F. Hertelendy, *Progesterone withdrawal: key to parturition.* Am J Obstet Gynecol, 2007. **196**(4): p. 289-  
697 96.
- 698 10. Ojasoo, T., et al., *Binding of steroids to the progesterin and glucocorticoid receptors analyzed by correspondence*  
699 *analysis.* J Med Chem, 1988. **31**(6): p. 1160-9.
- 700 11. Philibert, D., et al., *From RU 38486 towards Dissociated Antiglucocorticoid and Antiprogestone.* Frontiers of  
701 Hormone Research, 1991. **19**: p. 1-17.
- 702 12. Karalis, K., G. Goodwin, and J.A. Majzoub, *Cortisol blockade of progesterone: a possible molecular mechanism*  
703 *involved in the initiation of human labor.* Nat Med, 1996. **2**(5): p. 556-60.
- 704 13. Ogle, T.F. and B.K. Beyer, *Steroid-binding specificity of the progesterone receptor from rat placenta.* J Steroid  
705 Biochem, 1982. **16**(2): p. 147-50.
- 706 14. Hoffmann, B., et al., *Investigations on hormonal changes around parturition in the dog and the occurrence of*  
707 *pregnancy-specific non conjugated oestrogens.* Exp Clin Endocrinol, 1994. **102**(3): p. 185-189.
- 708 15. Nishiyama, T., et al., *Immunohistochemical study of steroidogenic enzymes in the ovary and placenta during*  
709 *pregnancy in the dog.* Anat Hist Embryol, 1999. **28**(2): p. 125-129.
- 710 16. Onclin, K., B. Murphy, and J.P. Verstegen, *Comparisons of estradiol, LH and FSH patterns in pregnant and*  
711 *nonpregnant beagle bitches.* Theriogenology, 2002. **57**(8): p. 1957-1972.
- 712 17. Kowalewski, M.P., et al., *The Dog: Nonconformist, Not Only in Maternal Recognition Signaling.* Adv Anat Embryol  
713 Cell Biol, 2015. **216**: p. 215-37.
- 714 18. Kowalewski, M.P., *Selected comparative aspects of canine female reproductive physiology,* in *Encyclopedia of*  
715 *Reproduction,* M.K. Skinner, Editor. 2018, Academic Press. p. 682-691.
- 716 19. Vermeirsch, H., P. Simoens, and H. Lauwers, *Immunohistochemical detection of the estrogen receptor- $\alpha$  and*  
717 *progesterone receptor in the canine pregnant uterus and placental labyrinth.* The Anatomical Record, 2000. **26**.
- 718 20. Kowalewski, M.P., et al., *Canine Endotheliochorial Placenta: Morpho-Functional Aspects.* Adv Anat Embryol Cell Biol,  
719 2021. **234**: p. 155-179.
- 720 21. Kowalewski, M.P., et al., *Canine placenta: a source of prepartal prostaglandins during normal and antiprogestin-*  
721 *induced parturition.* Reproduction, 2010. **139**(3): p. 655-64.
- 722 22. Kowalewski, M.P., M. Tavares Pereira, and A. Kazemian, *Canine conceptus-maternal communication during*  
723 *maintenance and termination of pregnancy, including the role of species-specific decidualization.* Theriogenology,  
724 2020. **150**: p. 329-338.
- 725 23. Concannon, P.W., et al., *Parturition and Lactation in the Bitch: Serum Progesterone, Cortisol and Prolactin.* Biology  
726 of Reproduction, 1978. **19**(5).
- 727 24. Veronesi, M.C., et al., *Correlations among body temperature, plasma progesterone, cortisol and prostaglandin*  
728 *F2alpha of the periparturient bitch.* J Vet Med A Physiol Pathol Clin Med, 2002. **49**(5): p. 264-8.
- 729 25. Olsson, K., et al., *Increased plasma concentrations of vasopressin, oxytocin, cortisol and the prostaglandin F2alpha*  
730 *metabolite during labour in the dog.* Acta Physiol Scand, 2003. **179**(3): p. 281-7.
- 731 26. Zone, M., et al., *Termination of pregnancy in dogs by oral administration of dexamethasone.* Theriogenology, 1995.  
732 **43**(2): p. 487-494.
- 733 27. Wanke, M., et al., *Clinical use of dexamethasone for termination of unwanted pregnancy in dogs.* J Reprod Fertil  
734 Suppl, 1997. **51**: p. 233-8.
- 735 28. Austad, R., A. Lunde, and O.V. Sjaastad, *Peripheral plasma levels of oestradiol-17 beta and progesterone in the bitch*  
736 *during the oestrous cycle, in normal pregnancy and after dexamethasone treatment.* J Reprod Fertil, 1976. **46**(1): p.  
737 129-36.
- 738 29. Gram, A., et al., *Elevated utero/placental GR/NR3C1 is not required for the induction of parturition in the dog.*  
739 Reproduction, 2016. **152**(4): p. 303-11.
- 740 30. Nowak, M., et al., *Gene expression profiling of the canine placenta during normal and antigestagen-induced*  
741 *luteolysis.* Gen Comp Endocrinol, 2019. **282**: p. 113194.
- 742 31. Chapman, K., M. Holmes, and J. Seckl, *11beta-hydroxysteroid dehydrogenases: intracellular gate-keepers of tissue*  
743 *glucocorticoid action.* Physiol Rev, 2013. **93**(3): p. 1139-206.
- 744 32. Seckl, J.R. and B.R. Walker, *Minireview: 11beta-hydroxysteroid dehydrogenase type 1- a tissue-specific amplifier of*  
745 *glucocorticoid action.* Endocrinology, 2001. **142**(4): p. 1371-6.
- 746 33. Seckl, J.R. and M.J. Meaney, *Glucocorticoid programming.* Ann N Y Acad Sci, 2004. **1032**: p. 63-84.
- 747 34. Kowalewski, M.P., et al., *Luteal and placental function in the bitch: spatio-temporal changes in prolactin receptor*  
748 *(PRLr) expression at dioestrus, pregnancy and normal and induced parturition.* Reproductive Biology and  
749 Endocrinology, 2011. **9**(109).
- 750 35. Gram, A., A. Boos, and M.P. Kowalewski, *Uterine and placental expression of canine oxytocin receptor during*  
751 *pregnancy and normal and induced parturition.* Reprod Domest Anim, 2014. **49 Suppl 2**: p. 41-9.

- 752 36. Kowalewski, M.P., et al., *Time related changes in luteal prostaglandin synthesis and steroidogenic capacity during pregnancy, normal and antiprogesterin induced luteolysis in the bitch*. Anim Reprod Sci, 2009. **116**(1-2): p. 129-38.
- 753 37. Graubner, F.R., et al., *Decidualization of the canine uterus: From early until late gestational in vivo morphological observations, and functional characterization of immortalized canine uterine stromal cell lines*. Reprod Domest Anim, 2017. **52 Suppl 2**: p. 137-147.
- 754 38. Concannon, P.W., J.P. McCann, and M. Temple, *Biology and endocrinology of ovulation, pregnancy and parturition in the dog*. J Reprod Fertil Suppl, 1989. **39**(0449-3087 ): p. 3-25.
- 755 39. Amoroso, E.C., *Placentation*, in *Marshall's Physiology of Reproduction*, A.S. Parkes, Editor. 1952, Longmans, Greens and Co: London, UK.
- 756 40. Tavares Pereira, M., et al., *Prostaglandin-mediated effects in early canine corpus luteum: in vivo effects on vascular and immune factors*. Reprod Biol, 2019. **19**(1): p. 100-111.
- 757 41. Kowalewski, M.P., et al., *Expression of cyclooxygenase 1 and 2 in the canine corpus luteum during diestrus*. Theriogenology, 2006. **66**(6-7): p. 1423-30.
- 758 42. Nowak, M., S. Aslan, and M.P. Kowalewski, *Determination of novel reference genes for improving gene expression data normalization in selected canine reproductive tissues - a multistudy analysis*. BMC Vet Res, 2020. **16**(1): p. 440.
- 759 43. Xie, F., et al., *miRDeepFinder: a miRNA analysis tool for deep sequencing of plant small RNAs*. Plant Molecular Biology, 2012. **80**(1): p. 75-84.
- 760 44. Nowak, M., et al., *Functional implications of the utero-placental relaxin (RLN) system in the dog throughout pregnancy and at term*. Reproduction, 2017. **154**(4): p. 415-431.
- 761 45. Gram, A., A. Boos, and M.P. Kowalewski, *Cellular localization, expression and functional implications of the utero-placental endothelin system during maintenance and termination of canine gestation*. 2017.
- 762 46. Kowalewski, M.P., et al., *Characterization of the canine 3beta-hydroxysteroid dehydrogenase and its expression in the corpus luteum during diestrus*. J Steroid Biochem Mol Biol, 2006. **101**(4-5): p. 254-62.
- 763 47. Tavares Pereira, M., et al., *Luteal expression of factors involved in the metabolism and sensitivity to oestrogens in the dog during pregnancy and in non-pregnant cycle*. Reprod Domest Anim, 2021.
- 764 48. Gram, A., et al., *Biosynthesis and degradation of canine placental prostaglandins: prepartum changes in expression and function of prostaglandin F2alpha-synthase (PGFS, AKR1C3) and 15-hydroxyprostaglandin dehydrogenase (HPGD)*. Biol Reprod, 2013. **89**(1): p. 2.
- 765 49. Gram, A., et al., *Canine placental prostaglandin E2 synthase: expression, localization, and biological functions in providing substrates for prepartum PGF2alpha synthesis*. Biol Reprod, 2014. **91**(6): p. 154.
- 766 50. Li, X., et al., *Effects of Ziram on Rat and Human 11beta-Hydroxysteroid Dehydrogenase Isoforms*. Chem Res Toxicol, 2016. **29**(3): p. 398-405.
- 767 51. Turpeinen, U., et al., *Determination of urinary free cortisol by HPLC*. Clin Chem, 1997. **43**(8 Pt 1): p. 1386-91.
- 768 52. Jafari, Z., et al., *The Adverse Effects of Auditory Stress on Mouse Uterus Receptivity and Behaviour*. Sci Rep, 2017. **7**(1): p. 4720.
- 769 53. Li, Q.N., et al., *Glucocorticoid exposure affects female fertility by exerting its effect on the uterus but not on the oocyte: lessons from a hypercortisolism mouse model*. Hum Reprod, 2018. **33**(12): p. 2285-2294.
- 770 54. Rogers, S.L., et al., *Diminished 11beta-hydroxysteroid dehydrogenase type 2 activity is associated with decreased weight and weight gain across the first year of life*. J Clin Endocrinol Metab, 2014. **99**(5): p. E821-31.
- 771 55. Belkacemi, L., et al., *Altered placental development in undernourished rats: role of maternal glucocorticoids*. Reprod Biol Endocrinol, 2011. **9**: p. 105.
- 772 56. Togher, K.L., et al., *Epigenetic regulation of the placental HSD11B2 barrier and its role as a critical regulator of fetal development*. Epigenetics, 2014. **9**(6): p. 816-22.
- 773 57. Zheng, H.T., et al., *Progesterone-regulated Hsd11b2 as a barrier to balance mouse uterine corticosterone*. J Endocrinol, 2020. **244**(1): p. 177-187.
- 774 58. Zhu, P., et al., *Mechanisms for establishment of the placental glucocorticoid barrier, a guard for life*. Cell Mol Life Sci, 2019. **76**(1): p. 13-26.
- 775 59. Beitins, I.Z., et al., *The Metabolic Clearance Rate, Blood Production, Interconversion and Transplacental Passage of Cortisol and Cortisone in Pregnancy Near Term*. Pediatric Research, 1973. **7**(5): p. 509-519.
- 776 60. Fusi, J., et al., *The usefulness of claws collected without invasiveness for cortisol and dehydroepiandrosterone (sulfate) monitoring in healthy newborn puppies after birth*. Theriogenology, 2018. **122**: p. 137-143.
- 777 61. Groppetti, D., et al., *Maternal and neonatal canine cortisol measurement in multiple matrices during the perinatal period: A pilot study*. PLoS One, 2021. **16**(7): p. e0254842.
- 778 62. Thompson, A., V.K. Han, and K. Yang, *Spatial and temporal patterns of expression of 11beta-hydroxysteroid dehydrogenase types 1 and 2 messenger RNA and glucocorticoid receptor protein in the murine placenta and uterus during late pregnancy*. Biol Reprod, 2002. **67**(6): p. 1708-18.
- 779 63. Krozowski, Z., et al., *Immunohistochemical localization of the 11 beta-hydroxysteroid dehydrogenase type II enzyme in human kidney and placenta*. J Clin Endocrinol Metab, 1995. **80**(7): p. 2203-9.
- 780 64. Simmons, R.M., et al., *HSD11B1, HSD11B2, PTGS2, and NR3C1 expression in the peri-implantation ovine uterus: effects of pregnancy, progesterone, and interferon tau*. Biol Reprod, 2010. **82**(1): p. 35-43.
- 781 65. Kowalewski, M.P., *Luteal regression vs. prepartum luteolysis: regulatory mechanisms governing canine corpus luteum function*. Reprod Biol, 2014. **14**(2): p. 89-102.
- 782 66. Kowalewski, M.P., et al., *Progesterone receptor blockers: historical perspective, mode of function and insights into clinical and scientific applications*. Tierarztl Prax Ausg K Kleintiere Heimtiere, 2020. **48**(6): p. 433-440.
- 783
- 784
- 785
- 786
- 787
- 788
- 789
- 790
- 791
- 792
- 793
- 794
- 795
- 796
- 797
- 798
- 799
- 800
- 801
- 802
- 803
- 804
- 805
- 806
- 807
- 808
- 809
- 810
- 811
- 812
- 813
- 814
- 815

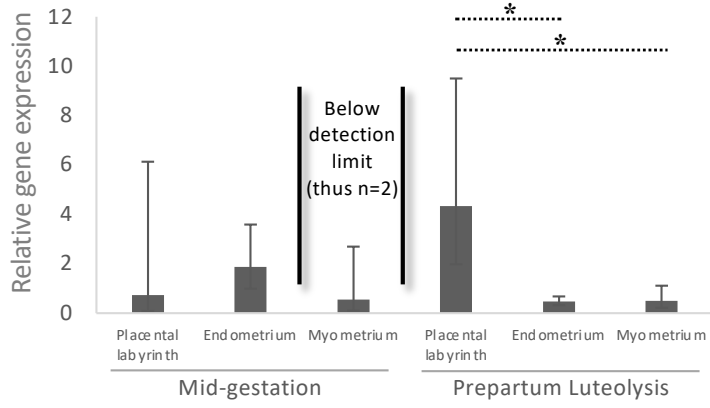
- 816 67. Sun, K., K. Yang, and J.R. Challis, *Differential expression of 11 beta-hydroxysteroid dehydrogenase types 1 and 2 in*  
817 *human placenta and fetal membranes.* J Clin Endocrinol Metab, 1997. **82**(1): p. 300-5.  
818 68. Bolt, R.J., et al., *Glucocorticoids and lung development in the fetus and preterm infant.* Pediatr Pulmonol, 2001.  
819 **32**(1): p. 76-91.  
820

**Fig. 1*****HSD11B1*****A.****B.*****HSD11B2*****C.****D.*****HSD11B1* vs *HSD11B2*****E.****F.**



**Fig. 2**

**A. *HSD11B1***



**B. *HSD11B2***

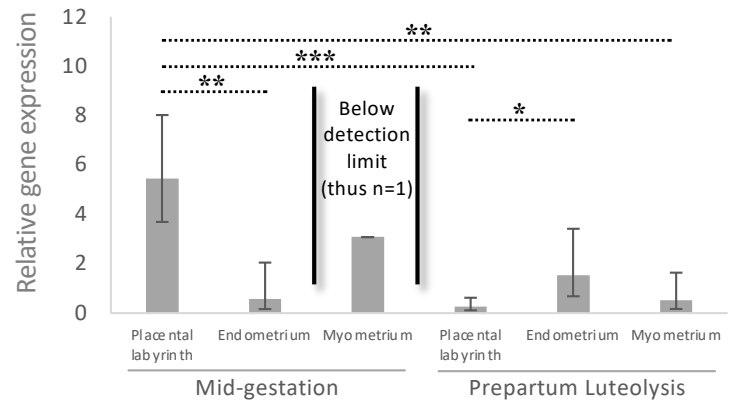


**Fig. 3**

**A.**



**B.**

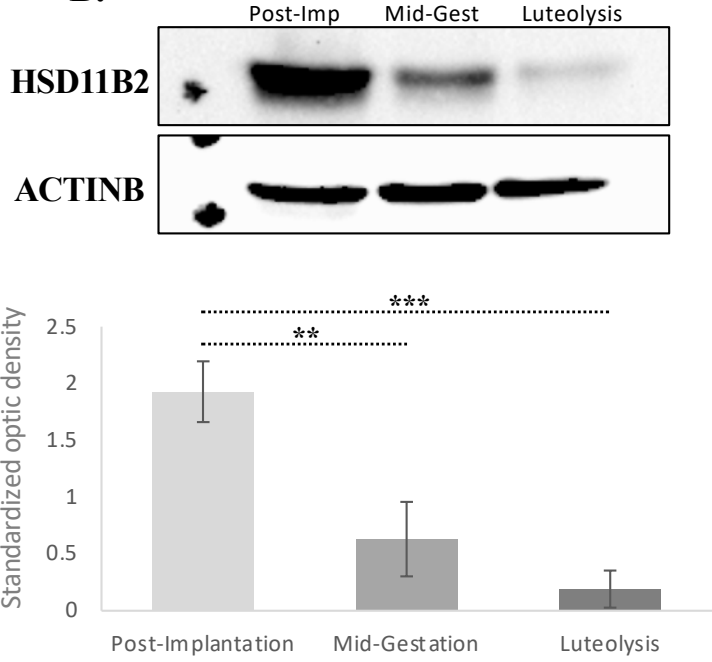
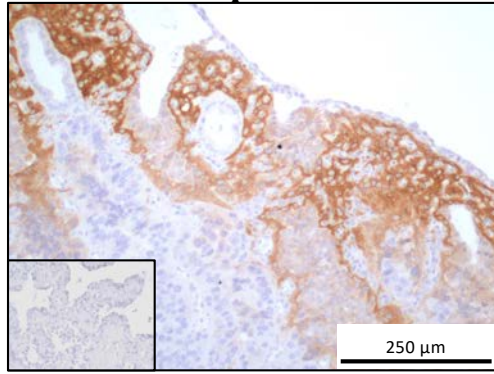
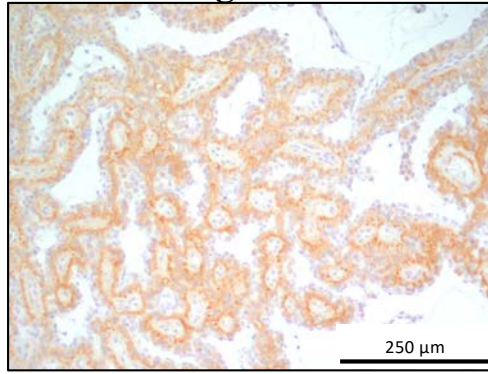


**Fig. 4**

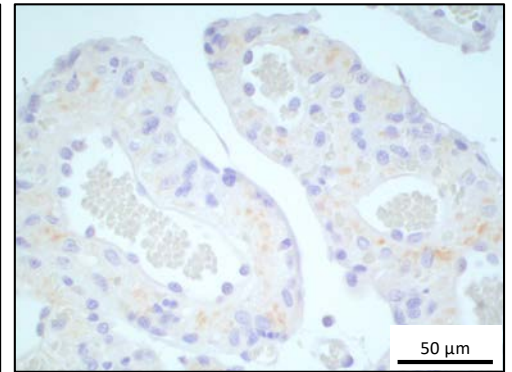
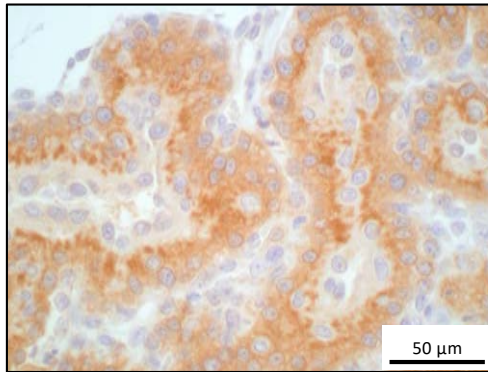
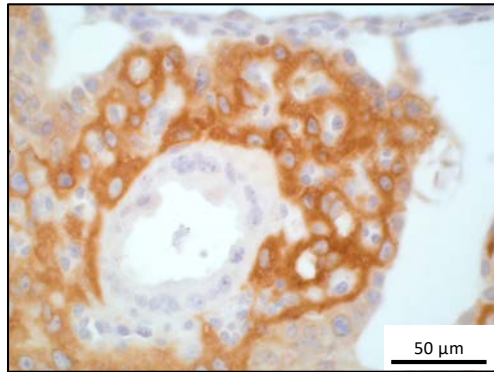
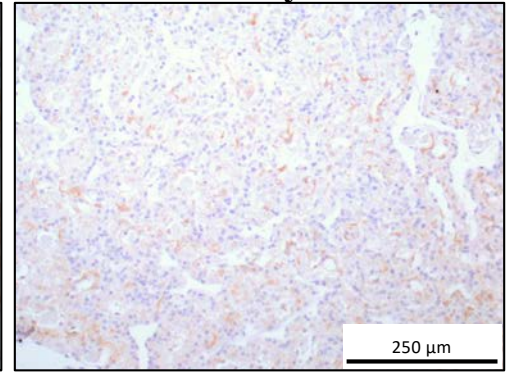
**A. Post-Implantation**



**Mid-gestation**



**Luteolysis**



**B.**

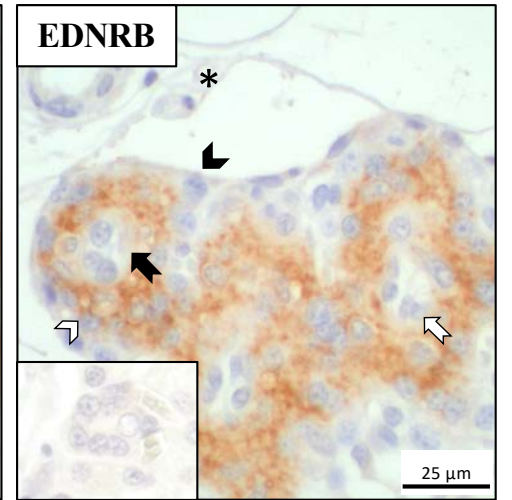
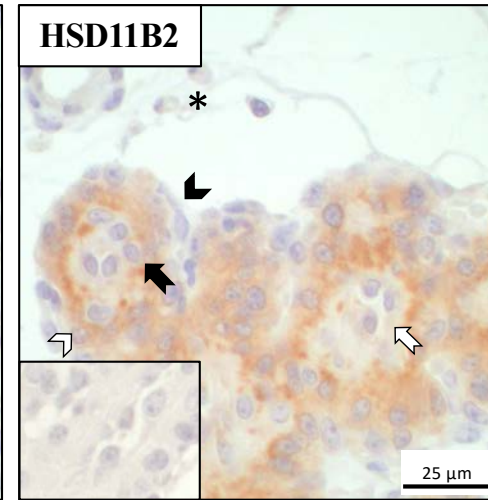
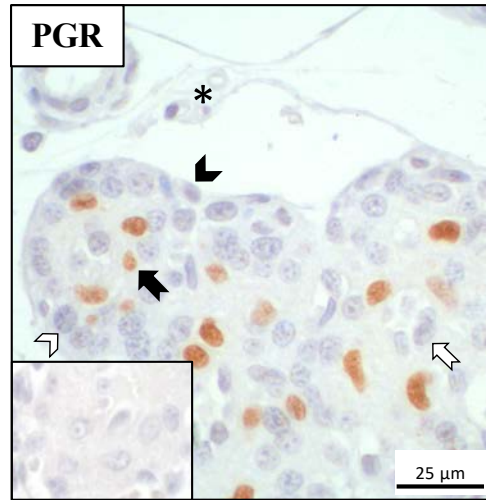


**Fig. 5**

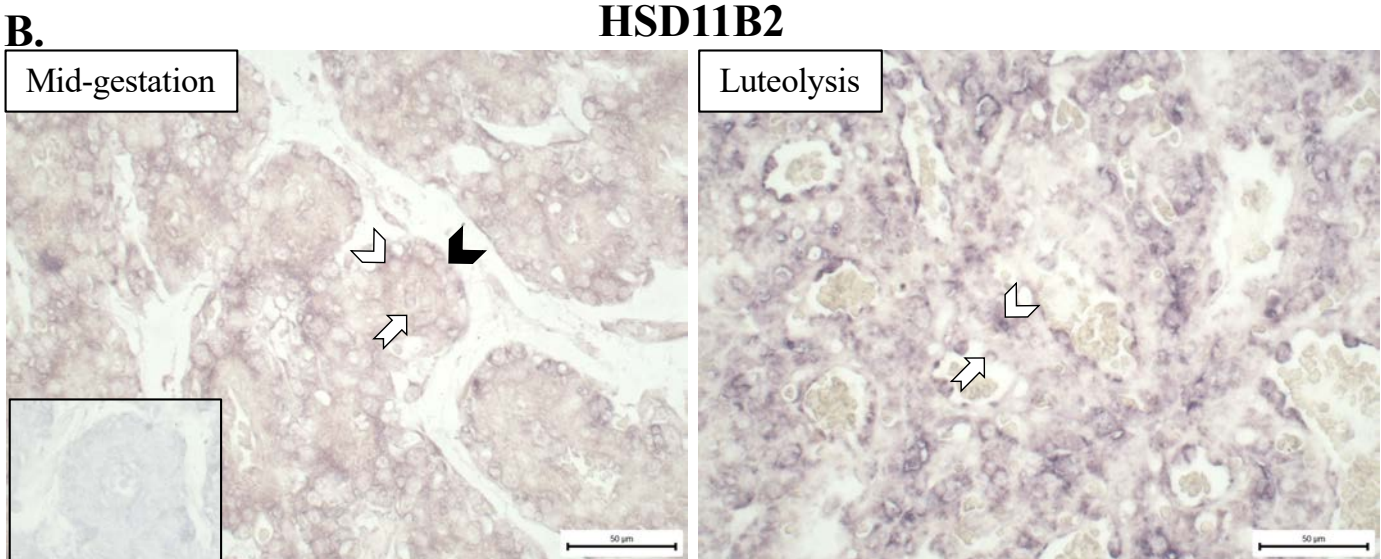
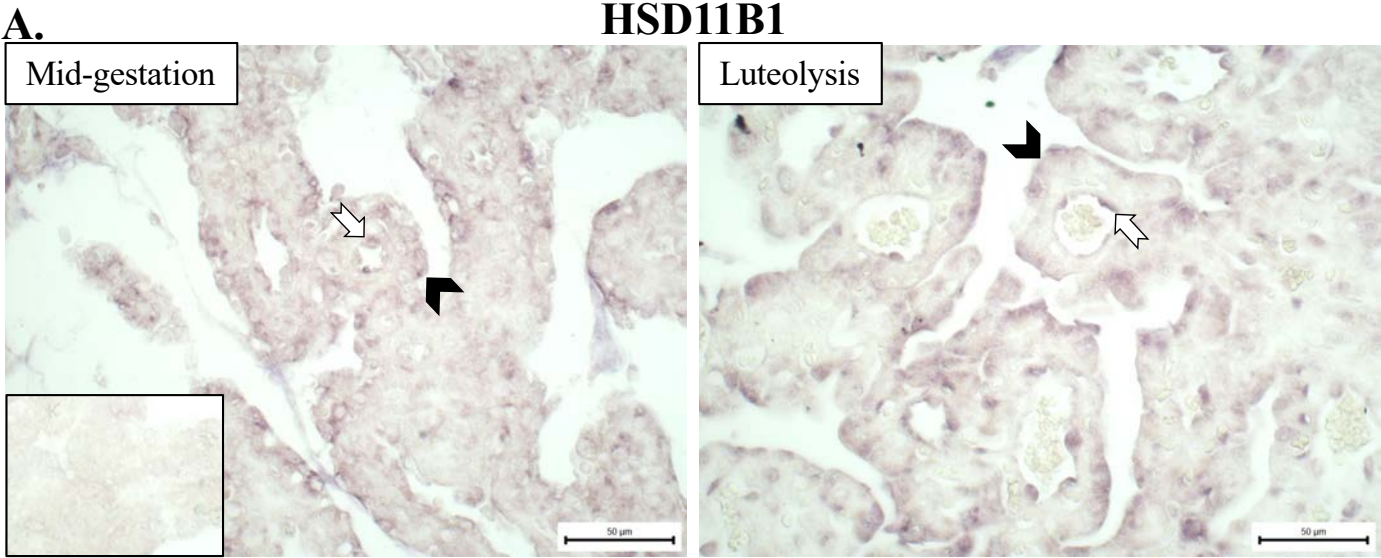


**Fig. 6**

